Conversion of Water Hyacinth into Graphene Containing Biochar for Effective Dye Removal from Textile Wastewater

Ahmednur Mohammed Hussein

A Thesis Submitted to

The Department of Chemical Engineering

School of Mechanical, Chemical and Materials Engineering

Presented in Partial Fulfillment of the Requirement for the Degree of Master's in Chemical Engineering (Specialization in Process Engineering)

Office of Graduate Studies

Adama Science and Technology University

February, 2024

Adama, Ethiopia

Conversion of Water Hyacinth into Graphene Containing Biochar for Effective Dye Removal from Textile Wastewater

Ahmednur Mohammed Hussien

Advisor: P. Selvakumar (PhD)

Co-Advisor:

A Thesis Submitted to

The Department Of Chemical Engineering

School of Mechanical, Chemical and Material Science Engineering

Presented in Partial Fulfillment of the Requirement for the Degree of Master's in Chemical Engineering (Specialization in Process Engineering)

Office of graduate studies

Adama Science and Technology University

February, 2024

Adama, Ethiopia

DECLARATION

I hereby declare that this thesis proposal entitled "**Conversion of Water Hyacinth into Graphene Containing Biochar for Effective Dye Removal from Textile Wastewater**" is my own work and has not been submitted to any university for similar purpose. The references used in this proposal are duly recognized by proper citations.

Name of the student	Signature	Date

ADVISOR'S RECOMMENDATION

I, the major advisor/supervisor of this research proposal, hereby certify that I have closely advised/supervised the student while developing this proposal and have read the draft thesis proposal entitled "**Conversion of Water Hyacinth into Graphene Containing Biochar for Effective Dye Removal from Textile Wastewater**" prepared under my guidance by **Ahmednur Mohammed Hussein** Therefore, I recommend the submission of the proposal to the department for further review and evaluation.

Major Advisor	Signature	Date

APPROVAL PAGE

I/we, the advisors of the thesis entitled "**Conversion of Water Hyacinth into Graphene Containing Biochar for Effective Dye Removal from Textile Wastewater**" and developed by Ahmednur Mohammed Hussein, hereby certify that the recommendation and suggestions made by the board of examiners are appropriately incorporated into the final version of the thesis.

Major advisor	Signature	Date

We, the undersigned, members of the Board of Examiners of the thesis by Ahmednur Mohammed Hussein have read and evaluated the thesis entitled entitled "**Conversion of Water Hyacinth into Graphene Containing Biochar for Effective Dye Removal from Textile Wastewater**" and examined the candidate during the open defense. This is, therefore, to certify that the thesis is accepted for partial fulfillment of the requirement of the degree of Master of Science in Chemical Engineering.

Chairperson	Signature	Date
Dr. Alemu Gizaw		20/02/2024
Internal examiner		Date
Dr.Sintayehu Mekuria		20/02/2024
External examiner	Signature	Date

Finally, approval and acceptance of the thesis is contingent upon submission of its final copy to the Office of Postgraduate Studies (OPGS) through the Department Graduate Council (DGC) and School Graduate Committee (SGC).

Department Head	Signature	Date
School Dean	Signature	Date
Office of Postgraduate Studies, Dean	Signature	Date

ACKNOWLEDGEMENT

I would like to acknowledge, express my sincere gratitude, and give praise to the almighty God who has supported me throughout the years. I also want to thank my esteemed advisor, P. Selvakumar (PhD), for his invaluable guidance and assistance, without which this research would not have progressed to this point. I have special thanks to my wife Mrs. Ameterehim Abdulkadir for her support and strive she provided me. Above all, I must express my heartfelt thanks to my mother Hamziya Ahmed , whose love, bravery, and support helped me get to the current level.

I am also very appreciative of my classmates' assistance with editing, their late-night responses, and their moral support. Lastly, I would like to express my sincere gratitude to everyone who contributed to this research work.

Table of Contents

LIST OF TABLES

LIST OF FIGURES

ABBREVIATIONS

AC	Activated Carbon
AOP	Advanced Oxidation Process
BC	Biochar
BOD	Biological oxygen Demand
COD	Chemical Oxygen Demand
CR	Congo Red
eAOP	Electrochemical Advanced Oxidation Process
FTIR	Fourier Transform Infrared spectroscopy
FWHM	Full Width Half Maxima
GCWHBC	Graphene Containing Water Hyacinth Biochar
MB	Methylene Blue
MDR	Multiple Drug-Resistance
MF	Micro Filtration
NF	Nano Filtration
NPs	Nanoparticles
PSO	Pseudo Second Order
PZC	Point of Zero Charge
RO	Reverse Osmosis
TDS	Total Dissolved Solid
TGA	Thermogravimetric Analysis
UF	Ultra Filtration
UV	Ultra Violet
WH	Water Hyacinth
WHBC	Water Hyacinth Biochar

XRD	X-Ray Diffraction
SEM	Scanning Electron Microscopy
DTG	Derivative Thermogravimetric

ABSTRACTS

An aquatic plant known as water hyacinth harms water bodies and endangers aquatic life. It is essential to use the latest innovations to convert this plant into a useful product. As a result, this plant was used to produce graphene-containing biochar, which was used in the removal of dye from textile waste water. Introducing graphene to biochar increased its application capacity for dye removal in an efficient and cost-effective manner. The physicochemical properties of graphene-containing biochar—which is produced from biological solid waste like water hyacinth—were greatly enhanced (e.g., surface area, surface functional groups, thermal stability, etc.). Thus, biochar containing graphene was utilized as an adsorbent to remove dyes from textile wastewater. In this research, the water hyacinth biochar was produced through slow pyrolysis and then modified by graphene. The product was characterized by different characterization techniques, such as XRD, FTIR, , BET, and TGA. Batch adsorption experiments were conducted in order to test the removal efficiency of Graphene containing water hyacinth biochar. The effects of different parameters such as adsorbent dosage, contact time, initial concentration, and pH on removal efficiency were studied. The PZC was found to be 6. The maximum removal efficiency achieved was 90.6% at the optimum conditions of pH=4, adsorbent dosage1g, concentration 40 mg/L and optimum time is180 min. The Langmuir adsorption isotherm is best fitted for this experiment (R^2 = 0.99413), and the pseudo-second-order kinetic model is best fitted (R^2 = 0.99423). The BET analysis result showed that the surface area of GCWHBC is 373.5 m^2/g. The synthesized graphene containing biochar was applied to real textile wastewater, providing the maximum adsorption efficiency of 63.2%. Finally, regeneration of the adsorbent was conducted to increase the efficiency of the adsorption cycle.

Key words: Graphene, water hyacinth, Graphene containing biochar, adsorption isotherms, adsorption kinetics

CHAPTER ONE

INTRODUCTION

1.1. Background of the study

Dyes are an important magnificence of pollutants, which are drastically utilized in many fields which include textiles, paper, plastic, leather-based, cosmetics, meals processing, wool, and printing (Yagub et al., 2014). The residual dyes in the wastewaters have posed a serious threat to the environment due to their high visibility, recalcitrance, and adverse effects on both the aquatic biota and human health (Mahmoud et al., 2012). Various physical, chemical, and biological removal techniques such as membrane separation process, coagulation, electrochemical and chemical precipitation, chemical oxidation, and aerobic or anaerobic microbial degradation have been used widely for the decontamination of dyestuffs in wastewater before their release into the environment (Annadurai et al., 2012).

Among these methods, adsorption has been recognized as one of the most effective, versatile, and innocuous technology for the treatment of dye-contaminated effluent (Sun et al., 2013). Activated carbon is often considered to be the most commonly used adsorbent for the decolorization of dyes in wastewater when compared to the other adsorbents such as agricultural solid wastes (Feng et al., 2012). However, activated carbon is still regarded as an uneconomic adsorbing material due to its expensive sources of raw materials and the high cost associated with its activation process.

Biochar, which has high specific surface area, excellent macroporous structure, enriched functional groups on its surface, as well as a lower cost of feedstocks and production process, appears to be an ingenious alternative to activated carbon (Tan, et al.2015). However, the original biochar still has limited removal ability to the dyes and other contaminants in wastewater, which limits its application to a certain extent. To enhance the adsorption capacity of biochar, many researchers prepared the biochar at high pyrolysis temperature (Mahmoud, et al. 2012).

Mahmoud et al. obtained the kenaf fiber biochar with improved pore structure by HCl treatment after pyrolyzing at1000 °C, which could be used to remove methylene blue

from wastewater (Mahmoud, et al., 2012). The iron oxide amended rice husk biochar charred at 950 ℃ was used to adsorb arsenate due to its high specific surface area in the study of Cope et al. (2014). Lee (2014) also prepared a $CoFe_2O_4$-modified biochar at 950 ℃ for Pb^{2+}andCd^{2+} removal from aqueous solution. In addition, temperatures at 600 °C and above are extensively chosen to prepare the original biochar in many other researches (Burhenne,et al 2014) Higher pyrolysis temperature may lead to higher adsorption capacity of contaminants onto the biochar by improving the physicochemical properties of biochar like specific surface area, pore structure, and cation exchange capacity (Ahmad, et al.,2012). But on the other hand, it could cause the loss of yield and surface functional groups, and higher energy consumption during the preparation, which may diminish the biochar‘s advantages of cost-effectiveness and resource conservation (Shen et al., 2012).

Therefore, it is urgent and necessary to specifically aim at effectively improving the adsorption capacity of the biochar prepared at relatively low temperature. Although biochar has many advantages, it produces by-products in the pyrolysis process, resulting in the reduction of specific surface area and functional groups of biochar, which further weakens the adsorption capacity of biochar to substances. Therefore, the performance of biochar needs to be improved by means of doping and modification (Mukherjee, et al 2017).

Water hyacinth (Eichornia crassipes), as one of the worst aquatic plants and the most aggressive invasive species in the world, has been a serious problem around the world due to its rapid spread and uncontrolled growth (Malik 2007). The conversion of the biomass of this invasive species into biochar for adsorbing pollutants in water could be a feasible and sustainable strategy for management of water hyacinth (Masto et al. 2013). The Awash River and Koka Lake in Ethiopia were the first places where water hyacinth was discovered in 1956 (Stroud 1994). With its disruptive effects on aquatic ecosystems, agriculture, fisheries, transportation, living conditions, and social structures in Ethiopia, it is known as "Emboch" in Amharic or "Bocee" in Afan Oromo. Koka Dam had the greatest plant population (308 plants/m^2), followed by Lake Koka (298 plants/m^2). (Tewabe,et al., 2017).

Several controlling mechanisms are available which include biological, physical (mechanical and manual removal), chemical control and integration of two or more control measures. Currently, a lot of attention is being paid to the development of processes for producing ethanol from biomass with high cellulose content. This type of ethanol, known as cellulosic ethanol, can be made from a variety of low-value materials, such as wood chips, grasses, crop residues, and municipal waste. The search for cellulosic substrates has accelerated recently and is still ongoing; some of these materials include water hyacinth and sunflower stalks, which are being investigated for their potential to produce ethanol in various laboratories (Rezania, et al., 2015). The plant can be used for a variety of purposes, such as the production of biofuel, biomass and energy, waste water treatment, compost and fertilizer, animal feed, and furniture. However, the application of water hyacinth for the energy sector is of particular interest (Rezania, et al., 2015).

Pollution as a result of industrial and human activity is becoming a concern for local and water authorities due to increased cost of water purification. One of the major contributors to water pollution is dye and pigment manufactures, pulp and paper, printing and textile industries. Reports from various researchers suggest that a total of $7x10^5$metric tons of dyes are produced annually worldwide from about 10000 commercially available dyes (Nadhini, et al., 2012).

The dying process produces huge volumes of colored water effluent. (Ratna et, al 2012) estimated that between 10-15% of dye is disposed of thereby making a highly colorful effluent. Discharge of huge volumes of dye effluent into rivers or lakes interferes with aquatic life and the dye compounds and their degradations products are known to be toxic or carcinogenic due to aromatic nature of most dyes (Kant, 2012). This has necessitated the need to develop viable dye effluent treatment methods.

1.2. Statement of the Problem

The aquatic biodiversity of the Awash River, which is the largest river in Ethiopia after the Nile River, is at extreme risk due to the aggressive water hyacinth, locally named Emboch. It causes a health risk to animals in the area and declines the economic activities of the river. Because of this problem, a huge amount of water hyacinth has been removed from the water surface and thrown to landfills without considering its economic use. Koka Dam had the greatest plant population (308 plants/m^2), followed by Lake Koka (298 plants/m^2). (Tewabe,et al., 2017).

According to the Ethiopian Electric Power Corporation (EEPC), this plant is causing operational disruptions at the three hydropower stations along the Awash River, which originates in Lake Koka (Stroud, 1994). Finding innovative technology to produce graphene containing biochar from water hyacinth for industrial applications is crucial to increasing its economic importance. One of the main sources of severe pollution problems worldwide is the textile industry and its waste waters containing dyes. 10–25% of the textile dyes are lost. During the dying process, 2–20% is directly discharged as aqueous effluents into different environmental components (Hao et al., 2000). The discharge of effluents containing dyes into water is undesirable due to the color of the dyes released and the breakdown products of dyes, which are toxic and carcinogenic to life, mainly because of the presence of carcinogens such as naphthalene, benzamine, and other aromatic compounds. If not treated, these dyes remain in the environment for a long period of time.

Hypothesis: The process of producing graphene containing biochar from water hyacinth for effective dye removal from textile waste water will be a promising research direction and play a vital role in solving an alarming environmental problem that puts both human beings and aquatic life in danger if the proposed methodologies and procedures are implemented properly.

1.3. Scope and Objective

1.3.1. Scope

Based on the proposed hypothesis, this research focused on the development, characterization, and study of the effect of graphene containing biochar on the textile industry waste water containing dye.

1.3.2. Objective

The main objective of this work is to produce graphene-containing biochar from water hyacinth biomass for the purpose of dye removal.

1.3.2.1. Specific Objectives

- ✓ To synthesize and characterize graphene-coated biochar from water hyacinth biomass and examine the removal capacity of the graphene-coated biochar for dye removal using synthetic wastewater.
- ✓ To investigate the effects of doze, pH, concentration, and time on removal efficiency or capacity.
- ✓ To conduct regeneration experiment in order to increase the efficiency of adsorption cycle.

1.4. Significance of the Study

The water hyacinth Eichhornia crassipes is one of the world‘s most invasive aquatic weeds, which causes serious environmental problems. Conversion of water hyacinth into useful products is a sustainable way to address the menaces created by them, along with an exploration of beneficial applications. It is important to focus on the conversion of water hyacinth into a climate-resilient product, biochar, and its applications in the textile industry. This work could be considered a milestone towards further optimization and field-level trials to enhance the effectiveness of the treatment of textile industry waste. The production of graphene-containing biochar from biological solid wastes and its characterization and potential use of graphene-containing biochar for dye-removing purposes have not been critically reviewed up to date. An effective way of using biochar for dye removal purposes in the textile industry is not only in this area of industry but also to protect the environment from damage. Generally, the significance of the research is to fill the gap in other chemical-based treatment of waste in the textile industry.

CHAPTER TWO

LITERATURE REVIEW

2.1. Textile industries wastewater: origin and composition

In case of textile wastewater, metal ions, dyes and its color are of the first concern due to their harmfulness to environment and people. The textile wastewater has a high color, high BOD/COD and salt (Total Dissolved Solids, TDS) load. The textile wastewater generated from cotton dyeing industry is extremely polluted due to presence of reactive dyes which are not readily amenable to biological treatment. Color water causes scarcity in the light which is essential for the development of the aquatic organisms. As result, it leads to an imbalance in the environment. To reduce the treatment cost of the river water which is used the purpose of drinking; it should not have any color and toxic compounds. So, before discharge of textile wastewater into river, many treatment processes including physical, chemical, biochemical, hybrid treatment processes have been developed to treat it in an economic and efficient way.

The components and structure of the textile industries vary from one factory or nation to another based on factors such as the type of fabric, seasonal couture trends, chemical application, abundance of fabric utilization, etc. Focusing primarily on the wastewater that is produced worldwide, the textile industry is among the most chemically intensive, using a large quantity of freshwater and dyes. The chemical industry's productivity determines whether the raw material is synthetic or natural. The discharged wastewater is a mixture of dangerous and toxic chemical solvents (Gupta, 2015). The sea is continuously permitted to receive various dissolved mineral salts and oils, ionic metals and their complexes, suspended solids, and a small number of non-biodegradable products. Inorganic metals and their complexes, which are either dissolved or present in other forms in actual water effluents, are among the main contaminants in the wastewater treatment industry. According to global reports, the most hazardous metals discovered in wastewater from textile industry manufacturing processes include cadmium, lead, zinc, chromium, arsenic, and others (Hussein, 2013). As is well known, the characteristics of dyes and their concentrations have been extensively documented in numerous manuscripts worldwide.

The complex solution made up of higher concentrations of various chemical pollutants, COD, BOD, heavy metallic ions and anions, nitrogen, biocides, dyestuffs or colorants, and mixed organic contaminants is examined when industrial effluents are discharged. The final result is a mixture of different materials. A dye's degree of toxicity can be determined by looking at its structures, functional group presence, and size. Specifically, the majority of chemicals with bleaching properties are retained by synthetic dyes, and azo dyes are a prime example of this. When azo dyes don't break down into aromatic amines, they can still cause mutations. However, the cleaved product of many azo dyes, benzidine, is the reason for their toxicity. Numerous tumors in humans and animals are caused by benzidine (Chung, 2016).

P-phenylenediamine is another component in azo dyes and a contact allergen. Numerous azo dyes, their reductively cleaved products, and chemically related aromatic amines have been shown to have an allergic effect on human health (Chung, 2000) . In addition to azo dyes, other processed dyes such as orange 3R and blue S, as well as different direct dyes like crystal violet and congo red, are also procured. These dyes are treated in an acidic, basic, or neutral medium to maintain a suitable pH. Both the precursor and successor compounds of dyes should be handled carefully because they contain chemicals that can cause cancer in living things.

2.2. Textile industries wastewater treatment methods.

Based on their basic principles and workings, treatment processes generally consist of three stages: physical, chemical, and biological treatment. The primary cause for concern, however, is the wide range of strong and stable industrial dyes and pigments that are the most contaminating substances in textile effluent. The primary components of these organic pollutants are heavy metal ions, salts, stabilizing agents, and surfactants, which enable them to stick to textile materials for extended periods of time despite abrasions, water washing, and laundry. The majority of dyes used today are even too powerful to be broken down by anaerobic or aerobic processes. Because of this, present researchers are making every effort to clarify contaminated wastewater and degrade contaminants for clean water through process improvisation, integration, optimization, and intensification.

2.2.1. Physico-chemical process

Before releasing wastewater for chemical processing or direct release into waterways, various physical processes use a specific step in the handling process. The purpose of preliminary treatment is to remove different types of tiny particles, suspended in the wastewater, primarily oils and lubricant liquids (Srebrenkoska,et al.,2014). After the aforementioned procedure, primary treatment, also known as physicochemical treatment, is provided by filtration or sedimentation, in which the sediments settle after being treated with specific chemical agents known as coagulants.

2.2.2. Sedimentation

This is an example of a common sub-physical process that separates materials in the mixture that contain dye. During the water treatment process, these suspended solids and wastes are uniformly segregated due to gravity. These dye-related particles are initially stirred up by a powerful solvent turbulence and then allowed to remain motionless for a while until all of the sediments have properly settled up against a barrier. This makes sense given that they are moving in the fluid in reaction to the forces acting on them, such as electromagnetism, gravitational force, and centripetal force (Classen,et al.,2013). This is completely a physical process where loss of dye or wastewater can be prevented. But this process is quite tedious and seems to be impossible when up scaling of these wastes comes in act (Behera,et al., 2021).

2.2.3. Flocculation/coagulation process

Coagulation merely results in the formation of flocculated agglomerates, or tiny molds, as a result of variations in the zeta potential on the surface area of/among the particles. Wastewater is treated with coagulants because it contains a significant amount of pollutants and impurities when it is released into waterways. To keep the system pure, some helpful iron coagulants such as ferrous sulfate, ferric chloride sulfate, and ferric chloride are added. Adsorbing the dyes and their byproducts is greatly aided by the use of other chemical coagulants like magnesium carbonate and hydrated lime (Mehta, 2013). Hence, coagulants that are added to solutions and vigorously mixed tend to precipitate, which traps organic pollutants and impurities (Hussain, et al., 2013). Similar to the sedimentation process, the mixture solution rested after being stirred, allowing all of the

precipitates to form and the trapped molecules to settle. To obtain clean water, these settled compounds can be further filtered out physically. Once more, unlike other chemical processes, this one does not explain the dissolved dyes and toxic pollutants.

2.2.4. Ion exchange process

As the name suggests, ion exchange process does include exchange of ions between a solid (resin/zeolite) and a liquid (water). But this technique is not so efficient in decolorizing the dyes in water treatment plants (Solmaz, et al., 2007). Actually, this process involves moving industrial wastewater over these ion exchange resins until all of their pores are saturated and clogged (Robinson, et al., 2001). The total cost of the process is sufficiently high even though very few dyes and pollutants can re-enter the solution or effluent (Crini, et al., 2019). Ionic floc is a large structured complex that forms when anionic or cationic dyes react with ion exchange resins, according to theory. Furthermore, there is an attempt to exchange ions between these hydrolyzed dyes and the active functional groups of the resins through strong ionic interaction, hydrogen bonding, or weak van der Waals forces. Ionic floc is a large structured complex that forms when anionic or cationic dyes react with ion exchange resins, according to theory. Furthermore, there is an attempt to exchange ions between these hydrolyzed dyes and the active functional groups of the resins through strong ionic interaction, hydrogen bonding, or weak van der Waals forces. In actuality, the kind and quantity of these interactions can affect how quickly dyes degrade (Deaconu,et al.,2016).

2.2.5. Adsorption process

Adsorption has gained a great deal of popularity in the modern era because of its flexibility and effective screening capabilities for removing contaminants and dirt from mixtures. The aim of this process is to create the most desired products with the fewest possible impurities. Similar to this, adsorption is frequently used in the textile industries' water treatment processes to filter out blended products. Adsorption and ion exchange are the two mechanisms that are used to explain decolorization. Several physio-chemical elements, such as the type of adsorbent, the type of adsorbate (dye), surface area, porosity, particle size, temperature and pressure, pH, contact time, etc., support this (Mohammadi, et al.,2018). Wang et al. (2008) proposed a fascinating theory regarding

the role of surface fluorinated TiO_2 (F-TiO_2) particles in the HF etching method's degradation of the zwitterionic dye Rhodamine B. When exposed to various particles under visible light irradiation, RhB experiences distinct structural compromisations. For example, when RhB is treated with F-TiO_2 and pure TiO_2, it goes through a rapid N-dealkylation process and a chromophoric ring cleavage, respectively (Wang, et al., 2008).

Jain et al. have reported on yet another degradation of the same dye RhB by TiO_2 NPs. Similar to this, when exposed to visible light, some non-biodegradable azo dyes, such as Acid Orange 7, break down into smaller, non-toxic fragments and adsorb onto the surface of CeO_2 NPs at different pH levels (Ji, et al., 2009). Jain et al. have reported on the degradation of RhB dye by TiO_2 nanoparticles, continuing the process (Jain, et al., 2008). Similar to this, when exposed to visible light, some non-biodegradable azo dyes, such as Acid Orange 7, are broken down into smaller, non-toxic fragments and adsorbed onto the surface of CeO_2 NPs at different pH levels (Ji, et al., 2009). Because clay is colloidal, it contributes to the race even in the competition of diverse adsorption catalysts. According to El Mouzdahir et al.'s research on Moroccan clay, Methylene Blue (MB) dye is more quickly degraded when the activated clay mineral is treated with nitric acid (El Mouzdahir, et al., 2010).

2.2.5.1. Activated carbon based adsorption process

Small, low volume pores are created by processing carbonaceous sources like AC, which enhance their surface area for effective adsorption in chemical reactions (Kumar, et al., 2016). Even this is frequently used to remove dyes, have decolorizing effects, adsorb cationic and anionic dyes, and to some extent, remove acidic and reactive dyes (Banat, 2004). It goes without saying that the density of the contaminants in the wastewater and the quality of the carbon determine how well the adsorption process works. When the same initial AC is recycled and applied in subsequent steps as it loses its efficiency, the rate of adsorption or decolorization also tends to decrease (Faria, et al., 2009). Thus, the dosage of AC or consumption duration can be increased to promote a quicker recovery of the desired product/compound. It is essential that used AC be properly channeled into water bodies because it may contain a film of concentrated acid or dyes that are toxic to aquatic life. From an application perspective, AC is frequently employed as a degrading

or catalytic agent from ancient times. Similar to how Martin et al. demonstrated how commercial AC degraded the textile dye Mordant Blue 9, causing surface modification and a shift in the dye's ionic strength (Martins, et al., 2015). Additionally, Gegel et al. assessed the AC formation process using Pisum sativum pea shells to extract Methylene blue dye from an aqueous solution (Geçgel, et al., 2013).

2.2.5.2. Membrane separation process

Today's industrial waste effluent treatment membrane-based separation technology is crucial to reducing pollution and producing clean, reusable water. Nowadays, a lot of research is being focused on material science and polymer chemistry, as these fields have the potential to develop new applications in membrane manufacturing and membrane integrated systems.

Membrane technology has quickly become more and more important because it helps separate various rigid textile dyes from effluent into finer ones. Numerous pertinent reports and applications have been published that address the removal of dyeing pollutants through the use of membrane filtration (MF), ultrafiltration (UF), nanofiltration (NF), and reverse osmosis (RO). When more dyes are washed through the permeate, MF functions similarly to a strainer that removes colloidal particles from the exhausted dye bath. Before the wastewater is released for the NF step in the dyeing process, MF is thought of as a pretreatment technique for the treatment of the auxiliary industrial wastewater. UF, on the other hand, demonstrates how simple and straightforward it is to treat secondary effluents while effectively eliminating a variety of macromolecules. In actuality, the permeate grade in UF is only intended for a few insignificant processes (such as cleaning or scrubbing) during recycling procedures as opposed to a few essential ones, such as the textile industry's dyeing of colored fibers (Lafi, et al., 2018).

2.2.5.3. Chemical oxidation process

This is the most often used chemical bleaching or decolorization technique. This is mostly because of its simple and straightforward application procedure. Hydrogen peroxide is the primary oxidizing agent (H_2O_2). Some method, such as ultraviolet light (UV), is required to initiate or activate this agent (Patel, et al., 2020). Many techniques for chemically lightening or decolorizing various rigid dyes vary depending on how H_2O_2

is used. Chemical oxidation causes the dye-containing effluents to lose their color and causes the dye molecules' aromatic rings to split. Even the most well-known Fenton's reagent (Fe^{2+}/H_2O_2) is highly regarded as the treatment option for extremely resistant wastewaters. Chemical oxidation causes the dye-containing effluents to lose their color and causes the dye molecules' aromatic rings to split. Even the most well-known Fenton's reagent (Fe^{2+}/H_2O_2) is highly regarded as the treatment option for wastewaters that are toxic to living biomass sources or exhibit high resistance to biological cure (Dafnopatidou, et al., 2007). Chemical separation has been demonstrated to be an effective method for decolorizing both soluble and insoluble dyes. It involves the use of either adsorption, absorption, or both processes to remove dissolved dyes from wastewater. A major issue that impedes the process is even the pH of wastewater that is adjusted during oxidation by Fenton's reagent and post-treatment pH adjustment before discharge.

2.2.5.4. Advanced oxidation process

2.2.5.4.1. Ozonation process

Because of its extremely unstable atomic structure, it is a very fine oxidizing agent after chlorine (Zhang, et al., 2019). Due to its high potential for oxidation, ozone can break down the membranes of microbial cells, aromatic compounds, SCN, CN^-, phenols, and chlorinated hydrocarbons, which can interfere with essential metabolism. This is injected in precisely the right amount into various dye products, depending on how many colors it can sustainably produce. Furthermore, throughout the course of the chemical reaction, COD (Chemical Oxygen Demand) exhausts all of the dissolved oxygen. However, ozonation only removes all the color and leaves behind any excess CODs that could have turned into harmful primary or secondary metabolites in wastes (Suryawan, et al., 2018).

2.2.5.4.2. Electrochemical advanced oxidation process (eAOP).

In actuality, this is the newest and most sophisticated method that has ever been made available to humans. Compared to other processes, it has a lot more lead points to withstand for a long time. This approach, in particular, addresses some radicals that deal with pollutants and organic wastes (Wang, et al., 2012).The various radical/ionic forms of dissolved oxygen, such as hydroxyl radical/ion, superoxide radical/ion, and oxide ions,

are produced when the solution is charged.

The hazardous organic dye molecules are primarily attacked by these dissolved active hydroxyl radicals (OH•), which then contribute to the chemical reaction that breaks them down into H_2O and CO_2, which are less toxic and more useful compounds in nature (Martinez, 2006). There are essentially two types of eAOPs when it comes to the process: direct and indirect.

2.2.6. Biological process used for textile wastewater treatment

Since the textile industries have long been engaged in an unrelenting race to the top, it is expected that in the near future, the pressure from demands for fiber consumption will increase threefold more than population growth. It is clear from the discussion above that various physicochemical processes have been successfully used in the market without any further thought. However, the environmental risks associated with post-treatment of the same process are greatest when it comes to the safe disposal of chemically treated sludge and secondary dye effluents and their reusability.

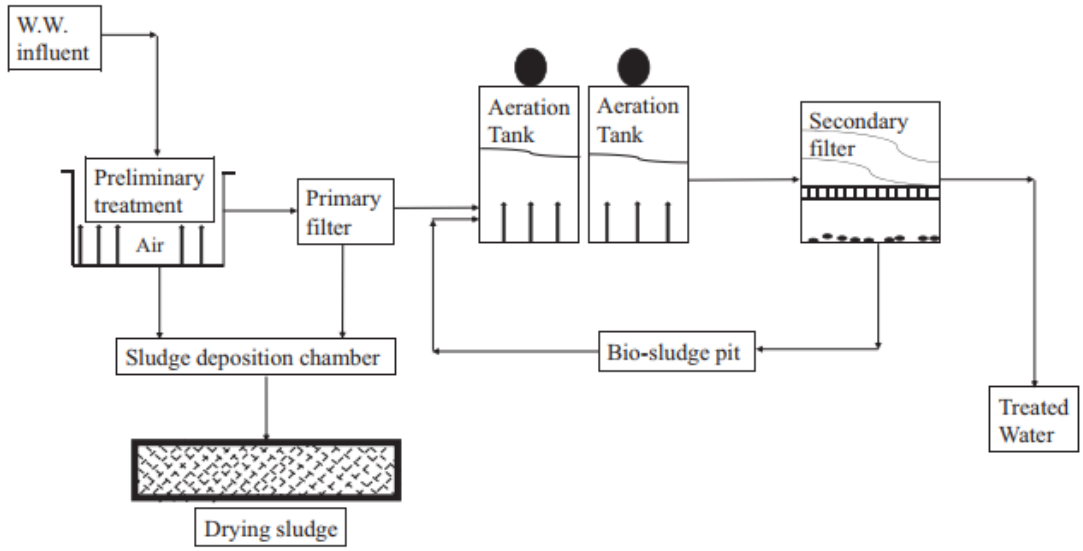

* W.W.= wastewater

Figure 2.1 Biological treatment of textile dyes (Behera, et al., 2021).

Despite the fact that numerous reports on the physicochemical methods of dye degradation and decolorization have been published, the most promising approach according to the current framework is thought to be biological treatment because of its

low cost, low sludge deposition, and environmentally friendly nature. The schematic representation of the biological treatment of textile dyes is shown in Fig. 2. Therefore, bioremediation which removes organic contaminants from the environment through the use of microorganisms, bacteria, plant extracts, and animal waste is typically taken into account (Khan, et al., 2020). Furthermore, using this method causes the bacteria to change into multiple drug-resistant (MDR) strains as they adapt to more toxic wastes. Techniques for enzyme-based remediation include riboflavin, laccases lignin peroxidases and azo reductases (Senan, 2004).

2.2.6.1. Microbial treatment (phycoremediation)

Microorganisms present in degraded dye effluents and their wastewater aid in the breakdown of those harmful macro-compounds into smaller, more basic elements. This treatment is now a broad, in-depth, and well-researched method that supports and enhances other chemically processed techniques. Furthermore, by preventing themselves from degrading, a wide range of living species and organisms are included in this treatment to improve the quality of the water, soil, and air. However, there are two phases to this process: anaerobic (without oxygen) and aerobic (with oxygen), during which time fungi and bacteria are crucial in breaking down the dangerous dyes. In 20 days of incubation at pH 8, Aragaw et al. achieved a higher reduction rate in COD (91.50%), BOD (91.9%), and TDS (89.1%) in decolorizing 82.6% of the textile dyes by different microalgae with 10% inoculums (Aragaw, et al., 2018).

2.2.6.2. Aerobic and anaerobic treatment

Bacteria involved in aerobic treatment produce the enzymes needed to break down organic pollutants. Kurthia species have been found to degrade and decolorize azo dyes and triphenylmethane dyes, such as malachite green, brilliant green, ethyl violet, etc., by more than 90% (Jamee, et al.,2019). Researchers found that, following biotransformation, the COD reduction of the triphenylmethane dye cell free extracts was greater than 88% for all dyes, with the exception of ethyl violet, which had a reduction of 70%. Reactive Blue 222 is an azo dye that has been biodegraded up to 96.88% and 95.23%, respectively, by two white rot fungi, P. ostreatus IBL-02 and P. chrysosporium IBL-03, through photo Fentonoxidation combined with aerobic biological treatment (Kiran, et al., 2013). A few

genera of Basidiomycetes aerobic bacterial strains also accompany azo dyes in order to remove them during the water treatment process (Pandey, et al., 2007).

2.3. Commericaly avialable textile dyes

Over 100,000 dyes are reported to be useable, with the textile industry being the primary application (Amalina et al., 2022c). As a result, it is expected that more than 300,000 tonnes per annum will be discharged into the waterways from the textile industry, excluding other sectors (Kadhom et al., 2020). The main characteristics of these effluents include higher levels of alkaline content, biological oxygen demand (BOD), chemical oxygen demand (COD), and total dissolved solids (TSS) with a concentration of dye/dm^3 below 1 g (Jesudoss et al., 2020). Adverse effects of dyes on plants and animals include skin irritation, carcinogenesis, decreased photosynthesis in aquatic plants, and disturbing the exquisite balance of the ecosystem (Amalina et al., 2019, Bagotia et al., 2020).

Dyes used in textiles are classified into two types, natural and synthetic dyes. Prior to the middle of the 19th century, dyes were derived from raw materials such as beet root. Typically, natural dyes are derived from plants, insects/animals, and minerals (Amalina et al., 2022d). They are generally less allergic and poisonous than synthetic dyes and produce biodegradable effluent (Benkhaya et al., 2020). Synthetic dyes are typically categorized as per their use, chemical structure, ionic forms, solution state, and colour (Chen et al., 2019). The most effective method for organizing dyes is their chemical structure, which provides numerous advantages (Nyoo et al., 2021). Synthetic dyes are formulated to meet current biological and physical resistant colouring agent requirements (Zubair et al., 2021). Thus, synthetic dyes are being established and gradually replacing natural dyes, especially in the textile and fabric industries (Zhou et al., 2019).

Generally, synthetic dyes contain several dyes in each category, including anionic, cationic, and non-ionic (Amalina et al., 2022c). Anionic dyes include direct, reactive, and acid dyes; cationic and non-ionic dyes include base and dispersed pigments, respectively (Kadhom et al., 2020). For instance, methylene blue is a widely used dye in the textile sector and other chemicals, medicinal, and biological applications (Nedjai et al., 2021). Methylene blue is a cationic stain with a complex structure, making it challenging to

remove. Similarly, methyl orange is used in numerous industries and has the same molecular weight as methylene blue (Rattanapan et al., 2017). The molecular structure of the multiple dyes is depicted in Table 1. In addition to methyl orange, methyl red is an azo dye with considerable molecular weight and numerous barriers to remove; many additional acidic and basic dyes exist and must be discarded.

Table 2.1. Organic dyes and their Chemical structure (Amalina, et al., 2022)

Name	Chemical Structural	Formula	Molecular weight(g/mole)	Density(g/cm^3)
Methylene blue	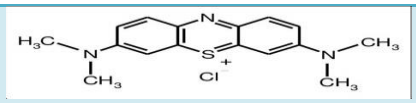	$C_{16}H_{18}ClN_3S$	319.85	0.98
Methyl orange	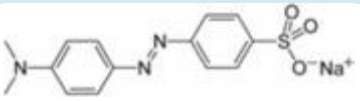	$C_{14}H_{14}N_3NaO_3S$	327.33	1.28
Methyl red	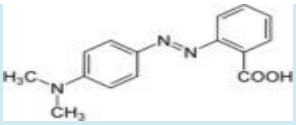	$C_{15}H_{15}N_3O_2$	269.304	0.791
Malachite green	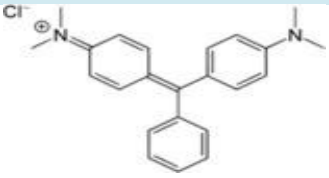	$C_{23}H_{25}N_2$	364.911	1.0448
Reactive Black 5	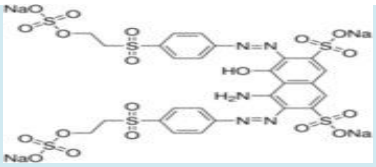	$C_{26}H_{21}N_5Na_4O_{19}S_6$	991.8	1.21
Congo red	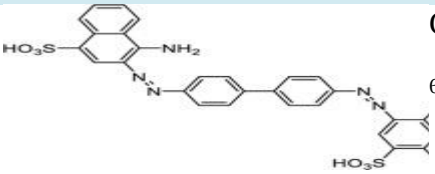	$C_{32}H_{22}N_6Na_2O_6S_2$	696.665	0.995
Rhodamine B	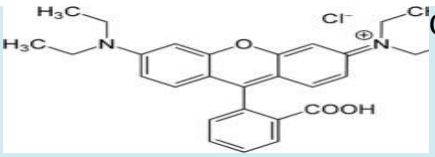	$C_{28}H_{31}ClN_2O_3$	479.02	0.79

Safranin	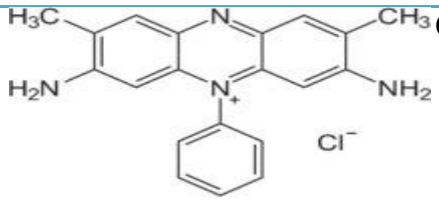	$C_{20}H_{19}ClN_4$	350.85	0.98

2.4. Biochar

Biochar is a carbon rich charcoal that is formed by the pyrolysis (thermal decomposition) of organic biomass or agricultural residues which is used as soil amendment (Xiao et al. 2014). It is composed of carbon (C), hydrogen (H), oxygen (O), nitrogen (N), sulphur (S) and ash in different proportions.

During the production of biochar, bio-oil and gases such as hydrogen is also produced that can be used for energy sources to power homes or automobiles. Lehmann (2007) and Powlson et al. (2011) suggested that application of biochar in the soil not only improve soil quality and nutrient cycling but it also poses the greatest potential for the long-term sequestration of carbon (C). Biochar has the capacity for remediation of contaminated soil and provides additional benefits to the environment.

2.5. Biochar: General characteristics

2.5.1. Physical properties

The physical properties of biochar directly depend on the biomass nature and pyrolysis conditions (including biomass pretreatment and handling). More specifically, attrition, cracks formation, and microstructural rearrangement occur during different pyrolysis processes, altering the biomass‘s original structures at various degrees (Downie et al., 2012). As the pyrolysis process continues, feedstock mass is reduced (i.e., volatile organics are released), resulting in disproportional amount of volume decrease or biomass shrinkage. At the end of pyrolysis step, C and mineral skeletons resembling the basic structure and porosity of the original biomass are formed. This physical modification has been confirmed by the existence of the identified plant cellular structures within coals and woods-derived biochar, contributing for most of the biochar macroporosity (Downie et al., 2012). Overall, biomass pretreatment, reaction temperature, heating rate, reactor type and dimension, the carrier/purge gas flow rate, residence time, pressure, and biochar

post modification methods are the main operating parameters shaping the physical structure of biochar produced via pyrolysis. For example, fast pyrolysis of biomass delivers biochar with low surface area. An ideal biochar physical structure could be developed by increasing reaction temperatures up to a point that any further temperature elevation triggers deformation. According to (Downie et al. 2012), biochar formed at ≤400°C had high aromatic hydrocarbon contents and were highly disorganized in amorphous mass. Like pyrolysis process conditions, the physical characteristics of the biomass also directly depend on the biomass chemical compositions. The thermal decomposition of organic materials starts at >120°C. More specifically, hemicellulose, cellulose, and lignin decompose at 200-260°C, 240-350°C, and 280-500°C, respectively (Downie et al., 2012).Therefore, the reactivity and physical structure modification degrees are impacted by the ratios of these components during pyrolysis process. On the other hand, the biochar physical structure could also be impacted by the ash ratio (i.e., inorganic components) through ash sintering of fusion under pyrolysis process (Downie et al., 2012).

Micropore volume could be improved through extending biomass pyrolyzing at higher reaction temperatures, providing the required activation energies and time for reaction completion, i.e., greater structural organization in biochar molecule (Downie et al., 2012). Typically, specific surface area of the biochar rapidly enlarges when pyrolysis temperature exceeds a certain value (for example 400°C) resulting in the thermal condensation of organic matters and formation of micropores (Li et al., 2019c).

2.5.2 Particle-size distribution

The rigidity of the biomass against shrinkage and attrition during pyrolysis process determined the biochar particle size. Generally, the particle sizes of the produced biochar are smaller than those of the un-pyrolyzed biomass. However, agglomeration may occur during pyrolysis process, leading to the formation of biochar with larger particle sizes than the starting biomass (Cetin et al., 2004). Post-mechanical stresses (e.g., during handling) may also occur, crumbling biochar that is more susceptible than the original biomass. Biochar particles with smaller size distributions could be obtained through slow pyrolysis with a heating rate of 5-30°C/min. Particle size has inverse correlation with

reaction temperature. For example, it has been observed that the tendency for formation of smaller size particles in biochar is increased by increasing reaction temperature from 450°C to 700°C (Downie et al., 2012). This could be attributed to the increased vulnerability to attrition due to reduced tensile strength in biochar.

2.5.3. Density

Apparent or bulk density and solid density could be considered in respect to determination of biochar physical properties. Typically, an increase in bulk density accompanies with a decrease in solid density. In general, solid density (i.e., the degree of C structure packing) of biochar is higher than that of the original biomass as the result of the volatile and condensable compounds release and formation of graphitic crystallites (Downie et al., 2012). Solid density of biochar increases with increasing the pyrolysis temperature (independent of the heating rate), hence causing higher shrinkage of solid matrix and the degree of carbonization .In contrast, biochar has lower bulk density (typically, ranging 0.3-0.43 g/cm^3) due to biomass drying and carbonization, compared to the wood precursor. However, bulk density of biochar (activated carbon) could be as high as 0.50 g/cm^3 and 0.75 g/cm^3 for gas adsorption and decolorization applications, respectively (Downie et al., 2012).

The availability of micropores within biochar increases its density, compared to macro- and mesopores (Downie et al., 2012). It should be noted that there is no strong correlation between pyrolysis temperature and biochar bulk density.

2.5.4. Mechanical strength

Biochar solid density and its level of aromaticity and crystallinity determine its mechanical strength. In another word, the mechanical stability directly correlates with density and hence, inversely with the porosity. The assessment of mechanical strength of paralyzed biochar was a topic of only few studies (Das et al., 2015).

2.5.5. Chemical properties

Any pyrolysis process could chemically manifest the biomass to form biochar with diverse properties. The properties of biochar are mainly determined by feedstock type and pyrolysis temperature. Typically, with the increase in the pyrolysis temperature,

biochar yield exponentially decreases whereas alkalinity (pH) of biochar shows a linear increase (rate, 0.5-1.4/100°C) (Li et al., 2019c). The elevation of pH is attributed to the thermal decomposition of hydroxyl bonds and other weak bonds within the biochar structure under high temperatures. In contrast, cation exchange capacity of biochar shows an inverse relationship with pyrolysis temperature due to the removal of acidic functional groups (Li et al., 2019c). Generally, biosolids-derived biochars have the highest cation exchange capacity because biosolids are rich in minerals (e.g., P, Mg, Ca, Na, and K) which promote the formation of O-containing functional groups on the surface of biochar during pyrolysis (Agrafioti et al., 2013).

2.6. Factors affecting properties of biochar

The reaction conditions during the pyrolysis process are mainly responsible for producing biochar. The factors such as feedstocks, temperature, size of the particle, heating rate, etc mainly influence biochar properties (Yaashikaa,et al., 2020).

2.6.1. Feedstocks

Biomass is considered as a complex solid material, composed of biological, organic, or inorganic material which was derived from living or living organisms. Biomass is characterized into two types (i) Woody biomass and (ii) Non-woody biomass. Woody biomass essentially includes tree residues and forestry residues (Tripathi,et.al 2016).

2.5.2. Carbonization temperature

The impact of pyrolysis temperature on such properties can be attributed to the influx of volatiles at high temperatures.

2.6.3. Residence time

Expanding the residence time at low pyrolysis temperature (300 ºC) brought about a slow decrease in biochar yield and reformist expansion in pH and iodine adsorption number of biochars. Nonetheless, expanding residence time at high pyrolysis temperature (600 ºC) had little impact on biochar yield or pH, while it diminished iodine adsorption number of biochars (Liang et al., 2006).

Pre-treating the biomass before pyrolysis influences biochar characteristics. The common pre-treatment methods available are immersing the raw materials in solution and particle

size reduction of biomass. The reduction of biomass particle size results in high biochar yield. For example, pine wood biomass was pre-treated by immersing the biomass in a dilute acidic solution. Pre-treatment methods such as nitrogen and metal doping can influence biochar production and solution pre-treatment such as soaking or steaming can influence the elemental composition and properties of biochar while the baking method can increase the carbon content and reduce the oxygen and moisture content of biochar(Yaashikaa et.al 2020).

2.7. Production Methodologies

Various production methods are used to produce biochar called bioenergy conversion biomass. Bioenergy conversion techniques are in general split into two distinct categories such as biochemical as well as thermochemical conversion governed by biological catalyst and organism while later one is governed by heat and chemical catalyst (Das and Veziroglu, 2001). First one is less expensive and eco-friendly compared to the second one, but yield and hydrogen production rate are quite low in the case of biochemical, which is the major constraint thermochemical conversion and is most popular and acceptable (Tripathi et al., 2016). The thermochemical approach is divided into combustion, pyrolysis and gasification.

2.7.1. Combustion

This is one of the oldest available processes used in biomass utilization in the form of energy. The stored chemical energy inside biomass is changed into heat in this process in the presence of oxygen/air directly ensures complete oxidation, and occur in the range of temperature 800 °C- 1,000 °C (Tripathi et al., 2016). The residue contains no or less unconverted flue gas energy and very low ash (McKendry, 2002a). It can be applied to any form of biomass means WH biomass too, feasible for biomass having moisture content is less than 50% also suitable for WH biomass (McKendry, 2002b). In many cases, direct combustion has been observed as not very effective and efficient. The pretreatment of biomass feedstock before combustion enhance process efficiency and increase overall process cost (Goyal et al., 2008).

2.7.2. Pyrolysis

This is an effective, economical, as well as efficient process to obtain heat/energy in char formation (Masto et al., 2013), also produced other value-added products, occurs in the range of temperature 400–1,200 °C depends on different operating parameters, but mainly favorable by low temperature as well as high residence time. It is based on the principle of thermal decomposition and exposed with limited oxygen contains various complex reactions in the reaction zone of the reactor. First, heating of biomass occurs, where molecules are divided and produced bio-oil on condensation (Lehmann and Joseph, 2015). This is used in the generation/production of BC under specified conditions (De Bhoumick et al., 2018). The process is involved with the decomposition of organic and lignocellulose matter thermally at high temperatures in the range of 200-700 °C with an inadequate supply of oxygen and controlled supply of air and gases (Poulose et al., 2018). As a result, after condensation biofuel is obtained while the solid residue is considered as BC. Based on different operating conditions like particle size, temperature, residence time, heating rate, and pressure are classified into six types as slow, fast, flash, intermediate, vacuum, and hydro pyrolysis among these commonly used are described below.

2.7.2.1. Slow Pyrolysis

It is specified by the low heating rate in the range of 0.1 to 1 °C/s having a prolonged residence time range in between 5 - 30 min or possibly 1 h, heated up to 400 - 550°C. It favours char formation along with a small quantity of liquid as well as gaseous products.

2.7.2.2. Fast Pyrolysis

It is characterized by a high-temperature range of 850–1,250 °C having low residence time 1-10 s with the heating range in the range 10-200 °C. It favors liquid product (60-75%), solid biochar (15-25%) and non- condensable gaseous products (10-15%). The other features are pH found in the range of 3.1 -3.59. The liquid product as bio-oil produced is highly corrosive in nature due to lower pH value. Thermal cracking also occurred and minimized exposure time of contact favors char formation.

2.7.3. Gasification

This thermo-chemical process takes places in the temperature range of 700-900°C produced gaseous fuels from carbonaceous biomass contents in the presence of medium such as air, nitrogen, oxygen, CO_2, steams or a mixture of these available gases (Reddy et al., 2014). Typically, in this process, outcomes contain around 85% gases, 10% char (solid) as well as 5% liquid products. The biomass partial oxidation is obtained by a little quantity of oxygen, which changes the final product properties .It recently becomes very efficient and widely method for H_2 production on the laboratory as well as large scale (Kumar et.al, 2019).

Tabble 2. 2. Fate of initial feedstock mass between products of pyrolysis processes (IEA 2007)

Process	Liquid (bio-oil)	Solid (biochar)	Gas (syngas)
Fast pyrolysis Moderate temperature (~500 °C) Short hot residence time (<2s)	75% (25% water)	12%	13%
Intermediate pyrolysis Low moderate temperature, Moderate hot vapour residence time	50% (50% water)	25%	25%

Slow pyrolysis Low-moderate temperature, Long residence time	30% (70% water) 5% tar (5% water)	35% 10%	35% 85%
Gasification High temperature (>800 °C)			

2.8. Feedstocks for Biochar production

The feedstocks of biochar are those materials which are abundantly available, considered as waste, or obtained at nil/low price. Specifically, biochar feedstocks are mainly prepared from forest and agricultural residues. Most of these resources are regarded as by-products or even wastes of harvesting and subsequent handling of crops including peanut, corn, sugarcane, oil palm and sorghum. To be precise, these resources generated in many countries are scarcely utilized and cause problems with disposal, and therefore can act as feedstocks for synthesis of biochar. For example, production of biochar from an invasive plant species can improve the management of that particular species and also solve problems associated with its disposal (Vijayaraghavan,et. al 2017). Additionally, seaweeds can also serve as a practical and cheap alternative feedstock for biochar as it rapidly reproduces and often create nuisances in world oceans. Recently, various feedstocks were identified to be suitable for biochar production, including wood chips, animal manures, marine algae, plant residues and municipal solid wastes (Hoslett, et al. 2019).

2.8.1. Water hyacinth

WH has been recently considered as a raw material for conversion into biochar, biohydrogen, bio methane, soil-biochar for crack propagation and various pollutant removals from waste water and water (Zhang et al., 2018). The advantageous addition of WH waste in the manufacturing of ecofriendly biochar used as an alternative for solving

strategy for solid waste management and further it helps in carbon sequestration process (Masek et al., 2013). In particulars, research is not sufficient in controlling of WH. Considerable research is still needed to control invasive plants through adapting new different ways such as the conversion of biomass into biochar. The concept behind WH biomass (both leaf, stem) in the form of biochar is more relevant as it contains cellulosic, hemicellulose, lignin in a proportional amount as compare to other mostly gained biomass such as rice straw, wood chips, sugarcane bagasse etc

Table 2. 3. Comparisons of biochars used in the adsorption of different textile dyes

Source of biochar	Adsorbate/dye	Removal efficiency	Reference
Casuarina seed biochar	Methylene blue dye	96.2%	Bharti et al. (2019)
Sludge	Methylene blue dye	73 %	Ahmad et al.(2020)
Rice Husk,	Methylene	71 %	Ahmad et al.(2020)
Cow Dung	Congo red	68%	Khan et al. (2020)
Rice Husk,	Congo red	80%	Khan et al. (2020)

2.9. Applications of biochar

2.9.1. As a tool for waste management

Each year a significant amount of waste is generated in the form of crop residues (e.g. rice straw, wheat straw, rice husk etc.), industrial waste (e.g. lumber, pulp, peelings and scrapes of fruits and vegetables, wood waste, etc.), forest residue (e.g. Dead wood, pole tree, logging residues), weed waste (e.g. Zizyphus sotundifolia, Calotropis procera, Lantana camera, etc.), animal waste (e.g. poultry litter, swine litter, etc.) and municipal solid waste (Walsh et al. 1999). Thus, the management of waste in such a way that is both sustainable to the environment and cost effective is extremely necessary to curb the nuisance of environmental pollution. Production of biochar helps in achieving the twin objective of both waste minimization and recovery of energy. Through pyrolysis, the weight and volume of initial biomass feedstock is reduced, thereby reducing the space required for its disposal.

Also the conversion of biomass waste into biochar and its subsequent addition in the soil helps maintain the soil nutrient which otherwise would have been removed from the soil. In addition, it helps in mitigation of GHG emissions such as methane and carbon dioxide that are generated from traditional waste disposal, processing and recycling operations (Woolf et, al., 2010). When the biomass is converted to biochar, 50% of carbon present in the biomass gets trapped in its structure which is more stable in nature as compared to the biomass which on degradation releases the carbon back in the atmosphere.

2.9.2. Treatment of wastewater

The most effective and widely used method for removal of organic compound such as pesticides, volatile compounds, chlorine, certain metal etc, is the use of activated carbon (biochar). Carbon filtering is a method which works on the principle of adsorption. Due to highly porous structure of biochar, it provides a large surface area, thereby providing a maximum surface area for the contaminants and impurities to interact with the active site of the biochar. For removal of sediments, volatile organic compounds (VOCs), odor, chlorine and taste, active biochar filters proved to be most effective (Lee et al. 2004) reported that due to the presence of anions like hydroxyl-and carboxyl-groups biochar functions as cation-exchanger. Also the classical graphite structure of carbon in biochar enables the carbon to connect with neighboring atoms or atoms from foreign molecules, which increases adsorption capacity.

2.10. Biochar Modification Techniques

Biochar alone was reported unable to effectively deal with the increasingly complex pollutant problems such as the simultaneous removal of mixed pollutants (Zhang, et al., 2018) and contaminants with trace concentrations (Fang, 2019) Therefore, the modification of biochar or combination with other substrate is considered to be a promising strategy to efficiently and economically manage the emerging environmental problems. The formation of graphene on the surface of biochar can increase the stability of the composite and acts as a very high potential active site. The porous structure and surface properties of biochar–graphene composites regulate the adsorption rate of pollutant molecules, thereby improving the adsorption performance (Zheng, et al 2021).

Several methods were used to alter the properties of biochar in order to change them for environmental implications. The two most popular techniques are physical and chemical modification. The most popular approach is chemical modification. It primarily consists of metal salts or oxidizing agents, acid and alkalinity modifications, and oxidizing agent modification.

2.10.1. Acid modification

Removing impurities like metals and adding acid functional groups to the surface of biochar is the primary goal of acid modification. According to Rajapaksha et al. (2016), common acids include hydrochloric acid, sulfuric acid, nitric acid, phosphoric acid, oxalic acid, and citric acid. The addition of 1 M hydrochloric acid to reed-derived biochar effectively reduced the amount of ash from 29.5% to 11.8% and supplied the hydrophobic adsorption sites for the adsorption process. The alteration made with the introduction of carboxylic, lactonic, phenolic, and carbonylic groups on the biochar surface made from bamboo (Liet al. (2014)). Additionally, acid modification can alter the surface area of biochar, and how different types and amounts of it affected the surface area acid concentrations. For instance, the reed-derived biochar's surface area grew from 58.75 to 88.35 $m^2.g^{-1}$ following 1 M of treatment with hydrochloric acid (Peng et al., 2016). However, following a 2% sulfuric acid treatment, the surface area of biochar made from rice straw dropped from 71.35 to 56.9 $m^2 g^{-1}$ (Yakout et al., 2015).

One common chemical agent that is used extensively is phosphoric acid. The biochar derived from rice straw showed a slight decrease in both surface area (from 522.5 to 517.1 m^2 g^{-1}) and total pore volumes (from 1.2 to 0.65 mlg^{-1}) upon phosphoric acid modification (Taha et al., 2014). The phosphoric acid concentration clearly affected the biochar's ability to adsorb substances (Zhou et al., 2017). Therefore, when using phosphoric acid as a modification agent, the ideal concentration should be chosen.

The concentration and kinds of acids, the feedstock, and the conditions of preparation are just a few of the variables that can affect the surface area of biochar. To look into the impact of the kinds and concentrations of acids on the biochar's surface, other parameters ought to remain the same. Currently, because of the various preparation circumstances and feedstock, it is too challenging to achieve a reliable outcome.

2.10.2. Alkaline modification

Increasing the surface area and the functional groups that contain oxygen is the primary goal of alkaline modification. Sodium hydroxide and potassium hydroxide are common alkaline agents. After modification with potassium hydroxide, the surface area rose from 14.4 to 49.1 $m^2.g^{-1}$), as well as the functional groups of biochar produced from municipal solid waste that were produced through pyrolysis, which led to an improved As(V) removal (Jin and others, 2014). The surface area of wheat straw-derived biochar produced by hydrothermal carbonization was reduced by hydroxide modification (from 4.4 to 0.69 m^2g^{-1}). Thus, it can be said that the impact of alkaline alteration on the biochar's surface area was also impacted by the kinds of feedstock and techniques for preparation. Compared to sodium hydroxide and potassium hydroxide are less caustic and additional financial (Cazetta et al., 2011).

The ratio of base to biochar, in addition to the various types of bases, can have a big impact on the properties of biochar. According to Shen and Zhang (2019), the characteristics of biochar were clearly affected by the mass ratio of biochar to KOH.

2.10.3. Oxidizing-agents modification

Oxidizing agents can be used to modify biochar in a way that increases the amount of functional groups that contain oxygen. According to Xue et al. (2012), the sorption capacity of lead can be increased by hydrogen peroxide modification of the peanut hull-derived biochar produced by hydrothermal carbonization by increasing the amount of oxygencontaining functional groups, particularly carboxyl groups.

According to Huff and Lee (2016), the addition of hydrogen peroxide resulted in a pH drop from 7.16 to 5.66 for the biochar made from pinewood and an increase in oxygen-containing functional groups. When the hydrogen peroxide content exceeded 10%, the modified biochar's adsorption capacity to methylene blue was reduced in comparison to the unmodified biochar. This suggests that biochar's adsorption capacity varied according to the pollutant target. Consequently, the characteristics of the targeted pollutants need to be taken into account before utilizing the modification of hydrogen peroxide. Like hydrogen peroxide, alteration by Potassium permanganate may also increase the functional groups that contain oxygen. In addition, biochar's surface area can rise from 101 to 205 m^2/g when potassium permanganate is modified. The addition of potassium

permanganate to biochar improved the adsorption capacity of biochar derived from hickory wood to Pb(II), Cu(II), and Cd(II) (Wang et al., 2015a).

2.10.4. Metal salts or metal oxides modification

Adsorption, catalysis, and magnetism properties can all be altered by utilizing metal salts or metal oxides. The development of metal salts or metal oxides was spurred by three factors.

(1) To increase the pollutants' targeted adsorption. For instance, because of the negative charge on its surface, biochar has a very low adsorption capacity to anionic dyes. Metal alteration can alter the characteristics of biochar's surface, enhancing the ability to adsorb anionic dyes even more;

(2) To repurpose charcoal. Because biochar is so tiny, it is challenging to recycle biochar from water when using biochar to eliminate contaminants from wastewater and water. Biochar's magnetic properties can be enhanced by adding iron salts or iron metal oxides, which can assist in the recycling of biochar;

(3) To improve biochar's catalytic properties. The persulfate activation process of biochar can be improved by adding metal salts or metal oxides to the material used in the metal-biochar composite's synthesis (Wang et al., 2018).

There are two methods for modifying metal salts or metal oxides: (1) mixing the metal salts or metal oxides with feedstock first, followed by pyrolyzing to create biochar; feedstock (2) is pyrolyzed to create biochar first, and then the biochar is soaked in metal oxides or salts under specific circumstances. Both approaches are extensively employed to alter biochar. Among the typical metals are manganese, iron, magnesium, and aluminum (Tan et al., 2016b).

Fe (III) modification of rice husk-derived biochar improved As(III) and As(V) removal (Samsuri et al., 2013). Likewise, the alteration of biochar made from swine dung by According to Liang et al., MnO_2 may improve the removal of Pb (II) and Cd (II). 2017a). To make marine macroalgae-derived materials more magnetic biochar was altered using the nano-composite Fe_3O_4 (Jung et al. (2016a). To improve biochar's catalytic properties, utilizing zerovalent iron at the nanoscale, the rice hull-derived Yan et al. (2015) discussed biochar. Corn straw was modified by Liu et al. (2015). Biochar utilizing iron and

discovered that the altered Tiny Fe_3O_4 granules covered the biochar, improving the effectiveness of phosphorus extraction from aqueous solutions.

210.5. Other modification methods

To increase the surface area of biochar, carbonaceous materials modification was also employed in addition to the previously mentioned modified methods. According to Zhao et al. (2011), carbon nanotubes and graphene are efficient at adsorbing organic pollutants and heavy metals. The cost of preparation can be further reduced by altering the biochar by adding graphene or carbon nanotubes to increase its surface area while reducing the amount of graphene or carbon nanotubes present.

2.11. Adsorption studies of dye removal using biochar

Adsorption has been found to be one of the best treatment processes for removing dye from water when compared to other conventional water treatment methods because it is less expensive, more affordable, more efficient, and requires less maintenance (Sirajudheen, et al., 2020). The fact that adsorption can treat large amounts of water and leaves no harmful residues is an additional benefit (Saxena, et al.2020). Additionally, an adsorbent may be recycled more than once and used in different treatment procedures (Da Silva, et al.2020). Common materials used for water treatment include silica gel, polymeric adsorbents, activated carbon, zeolites, and activated alumina. Because biomaterials have a low commercial value and are readily available, using them in place of conventional materials for adsorption processes is currently attracting the attention of many researchers (Deniz, 2013). The utilization of naturally-derived biopolymers as green adsorbents has gained considerable attention due to their hyper reactivity, chemical stability, and favorable physicochemical properties (Fan, et al., 2020). The main benefits and drawbacks of the various treatment options for removing dye from water are shown in Table 4.

Table 2.4. Advantages and Disadvantages of various treatment technologies for dyes removal from textile wastewater (Srivatsav, et al., 2020).

Treatment Technology for Dyes Removal	Advantages	Disadvantages
Membrane Processes	• Minor, valuable products can be recovered from the feed stream • Process can be easily "scaled-up" • No-phase changes involve between the feed and product stream • Eco-friendly as simple and non-toxic materials are used	• High flow rate has the potential to damage the membrane • This process results in membrane fouling effects. Regeneration and extensive cleaning are required. • High equipment cost
Biological Processes	• Almost all biodegradable organic matter is effectively removed • Efficient attenuation of color • Eco-friendly and a common wastewater	• Slow process • An optimal favorable environment is crucial • Biological sludge generation
	treatment mechanism	• Remediation of dye molecules is tough
Adsorption Processes	• Highly efficient process • Applicable for a wide variety of target contaminants • Treatment technology is easy to employ	• Deterioration of adsorbent performance when subjected to multiple operational cycles • Spent adsorbent is likely to be a hazardous waste • Regeneration of adsorbent material is expensive
Coagulation	• Reduced time for settling of suspended solids • Easy removal of fine particles • Effective in removing bacteria, protozoa, and virus	• High cost to spend for frequent monitoring and accurate dosing • Huge volume of sludge generation
Advanced Oxidation	• •OH radicals can treat a	• Fenton's reagent AOP

Processes (AOP)	wide range of organic material • Zero sludge production	results in iron sludge generation • High capital and maintenance costs are expected

2.12. Generally used and observed isotherms and kinetics

When it comes to dye removal, two commonly used and observed aspects are isotherms and kinetics. These concepts help in understanding the adsorption behavior of dyes onto various adsorbents or surfaces.

2.12.1. Isotherms

Isotherms describe the equilibrium relationship between the amount of dye adsorbed onto an adsorbent and the concentration of dye remaining in the solution at a constant temperature. They provide valuable information about the adsorption capacity and affinity of the adsorbent for the dye. Some commonly used isotherms in dye removal studies include:

Langmuir Isotherm: The Langmuir isotherm assumes a monolayer adsorption onto a homogeneous surface, where adsorption sites are energetically equivalent. It suggests that adsorption occurs through a reversible process and that there is no interaction between adsorbed dye molecules (Lorenc et al., 2007). The Langmuir isotherm equation is commonly expressed as:

$$\frac{C_e}{q_e} = \frac{1}{q_{max}} + \frac{C_e}{q_{max}} \dots\dots\dots\dots\dots\dots\dots\dots\dots\dots\dots\dots\dots\dots \; equ(2.1)$$

where C_e is the equilibrium concentration of the dye, q_e is the amount of dye adsorbed at equilibrium, q_{max} is the maximum adsorption capacity, and bq_{max} is the Langmuir constant related to the energy of adsorption.

Freundlich Isotherm: The Freundlich isotherm is an empirical equation that assumes a multilayer adsorption onto a heterogeneous surface. It implies that adsorption occurs on

sites with different energies and affinities (Lorenc et al., 2007). The Freundlich isotherm equation is typically represented as:

$$lnq_e = \frac{1}{n} lnC_e + lnK_F \ldots\ldots\ldots\ldots\ldots\ldots\ldots\ldots\ldots\ldots\ldots\ldots\ldots\ldots\ldots\ldots\ldots\ldots\ldots . equ(2.2)$$

Where q_e is the amount of dye adsorbed at equilibrium, C_e is the equilibrium concentration of the dye, K_F is the Freundlich constant related to adsorption capacity, and n is the Freundlich constant related to adsorption intensity.

2.12.2. Kinetics

Kinetics refers to the study of the rate at which adsorption occurs. It provides insights into the speed at which the adsorbent removes the dye from the solution. Two commonly observed kinetics models in dye removal studies (Xu, et al., 2016) are:

a. Pseudo-first-order Kinetics: The pseudo-first-order kinetics model assumes that the rate of adsorption is directly proportional to the number of unoccupied adsorption sites on the adsorbent. The equation is often expressed as:

$$(q_e - q_t) = logq_e - K_1 t/2.303 \ldots\ldots\ldots\ldots\ldots\ldots\ldots\ldots\ldots\ldots\ldots\ldots\ldots\ldots\ldots\ldots \text{equ}(2.3)$$

where qt is the amount of dye adsorbed at time t, qe is the amount of dye adsorbed at equilibrium, k1 is the rate constant of the pseudo-first-order kinetics, and t is the contact time.

b. Pseudo-second-order Kinetics: The pseudo-second-order kinetics model suggests that the rate of adsorption is proportional to the square of the number of adsorbed dye molecules. The equation is typically represented as:

$$t/q_t = 1/(k_2 q_e^2) + 1/q_e t \ldots\ldots\ldots\ldots\ldots\ldots\ldots\ldots\ldots\ldots\ldots\ldots\ldots\ldots\ldots\ldots\ldots\ldots\ldots\ldots\ldots\ldots\ldots\ldots \text{equ}(2.4)$$

Where q_t is the amount of dye adsorbed at time t, q_e is the amount of dye adsorbed at equilibrium, k_2 is the rate constant of the pseudo-second-order kinetics, and t is the contact time.

2.13. Removal mechanisms of dye from textile waste

Several complex interactions (both chemisorption and physisorption) between the adsorbate (dye) and adsorbent (biochar) are involved in the process of removing dyes from wastewater using biochar. Based on existing literature, it can be concluded that adsorption occurs through a combination of mechanisms, some of which are dominant and others which depend on the system's conditions. Mechanisms including pore-filling effect, van der Waals interaction, electrostatic interaction, chemical action, ion exchange, surface complexation, π-π interactions, and cation-π interactions could be important in the adsorption process, depending on the dyes, biochar, and solvent (Srivatsav, et al., 2020).

CHAPTER THREE

MATERIALS AND METHODS

The materials used, sample preparation procedures, and appropriate characterization techniques for the various experiments carried out in this research work are intended to be presented in this chapter. Experiments on desorption and regeneration were conducted after the adsorption process in a batch form. The materials used, the experimental procedures, and the characterization methods were divided into three sections for the sake of simplicity. The production of water hyacinth biochar is covered in the first section, and its modification is covered in the second. The methods for characterizing the graphene-modified water hyacinth biochar are explained in the third section.

3.1. Materials/Equipments and Chemicals

3.1.1. Materials/ Equipment's

Various materials and equipment were used for the synthesis, characterization, and physiochemical analysis of WHBC and GCWHBC. These included pipettes, gloves, analytical balances, water baths, pH meters, spatulas, hot plates, sieves, measuring cylinders, beakers, grinders, temperature-controlled reactors/ovens, magnetic stirrers, furnaces, flasks, vacuum pumps, and mixers. Additionally, tools like the powder X-ray diffraction (XRD), surface area and pore size analyzer (BET), ultraviolet–visible (UV–visible) spectrophotometer, and fourier transform infrared spectroscopy (FTIR) were employed for analysis.

3.1.2. Chemicals

The water hyacinth biomass for this study was collected from Koka dam area. All chemicals used in this study were of analytical grade. Graphene (C_2, 99.0%), hydrochloric acid (HCl, 37%), Ethanol (C_2H_6O, 96.0%), acetone (C_3H_6O, 99.5%). During the experimental work, the pH was adjusted using diluted (0.1 M) hydrochloric acid (HCl, 37.0%) and sodium hydroxide (NaOH, 99.0%), and distilled water. Graphene (C_2, 99.0 %) was used to modify water hyacinth biochar which is used as an adsorbent. The Chemicals mentioned above chemicals, hydrochloric acid (HCl, 37 %), ethanol (C_2H_6O 96.0%), acetone (C_3H_6O, 99.5%), deionized water, and other analytical chemical reagents

were used from Adama Science and Technology University (ASTU) Chemical Engineering Department Laboratory.

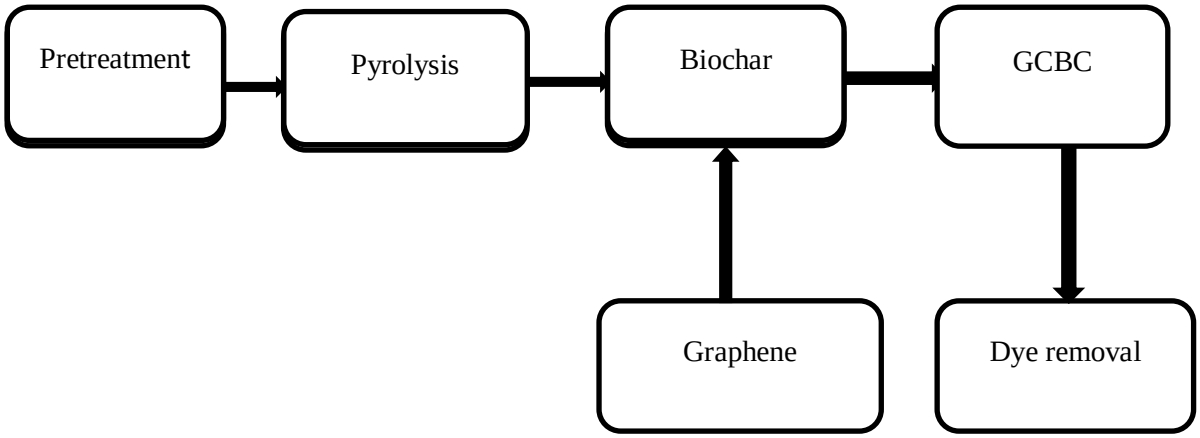

Figure 3. 1. Process flow diagram

3.2. Water hyacinth Pre-treatment

Pre-treating the biomass before pyrolysis influences biochar characteristics. The common pre-treatment methods available are immersing the raw materials in solution and particle size reduction of biomass. The reduction of biomass particle size results in high biochar yield. Accordingly water hyacinth biomass was pretreated by immersing the biomass in a distilled water to remove impurities. After washing, the water hyacinth biomass was dried in an oven at 80°C for 24h to reduce its moisture content. Then the size of water hyacinth biomass was reduced by cutter to facilitate for conversion process (pyrolysis).

3.3. Production of Water hyacinth Biochar

3.3.1. Slow Pyrolysis

Slow pyrolysis is a process of thermal decomposition of organic materials, such as biomass, in the absence of oxygen or with limited oxygen supply. It was heated up to 400 - 550°C. It favors char formation along with a small quantity of liquid as well as gaseous products (Mccarl et al., 2009). This method of synthesis was adopted in this work. The specific preparation method is as follows: Water hyacinth (WH) was collected from Awash river around Awash Melkasa town. WHs was washed with water three times to remove the attached dust, and then dried at 80 ºC for 24 h.

To control the size of biochar, the charred solid was passed through a 35 mesh sieve, and the resulting product is a biochar sample. The biochar was produced by slowly pyrolyzing the dried WHs in a pyrolyzer at 400 ºC, and 450ºC, 500 ºC and 550 ºC and 600 ºC for 1,2,3 h. After that the optimum temperature and optimum time for effective pyrolysis process were determined. According to the preliminary experiment test conducted, the water hyacinth biochar produced at 500 ºC and 1h showed relatively high adsorption efficiency and it is used for further experimental works. The products obtained at different temperatures were labeled as B_{400}, $B_{450,}$ B_{500}, B_{550} and B_{600} respectively, with the subscripts for each indicating different combustion temperatures. The slow heating rate and limited oxygen availability in slow pyrolysis promote the production of biochar, a carbon-rich solid residue.

3.4. Making graphene containing water hyacinth biochar

In this research work, BG composites were prepared by one-step dip coating. First, 7 g of biochar was immersed in 200 mL of the graphene nanometer suspension and stirred for 1 hour. During the biochar modification process, the graphene biochar composite was prepared in ratios of 1:10 to 1:2. Accordingly, the 1:7 ratio was selected because it showed the relatively best result for modification. After that, it was filtered by using a vacuum filtration pump with Watman filter paper. The mixture was then dried in an oven at 80 ℃ for 3 hours. The pre-treated biochar was pyrolyzed in a muffle furnace at 400 ℃, 450 ℃, 500℃, 550 ℃, and 600℃ to produce BG composites. The sample was then washed four times with deionized water to remove the water-soluble inorganic material. Finally, the biochar samples prepared were named B_{400}, B_{450}, B_{500}, B_{550}, and B_{600}, where B stands for biochar and subscripts 450, 450, 500, 550, and 600 indicate the temperatures at which the biochar was pyrolyzed.

3.5. Characterization

Biochar characterization was performed to determine the ability to remove pollutants or other applications. The structural and elemental analysis also helps to predict the impact of biochar on the environment. In this research work, numerous modern characterization techniques were implemented for characterizing biochar such as Fourier transform

infrared spectroscopy (FTIR), X-ray diffraction (XRD), Thermo-gravimetric analysis (TGA) and Brunauer-EmmettTeller (BET).

3.5.1. Fourier transforms infrared spectroscopy (FTIR)

FTIR spectroscopy is a vibrational technique for investigating the functional groups present on the surface of biochar. Using this, feedstock as biomass and their biochar was investigated with respect to distinct temperatures which is convenient in analyzing vibrational frequency changes of functional groups and gradual loss of functional group lignocellulosic (O-H straighten peak occur at 33,44 cm^{-1}, for unmodified water hyacinth biochar and 3322 for GCWHBC).

3.5.2. X-ray diffraction (XRD)

X-ray diffraction is a broadly relevant strategy to determine the crystallinity and structure of biochar**.** Thus, XRD patterns help in producing high quality, fast and non-destructive biochar with high adsorption efficiency. A SHIZMADZU XRD-7000 was used to record the powder X-ray diffraction (XRD) patterns of the WHBC AND GCWHBC. The XRD-7000 was operated at a scanning speed of 3 °/min for 2, with a scanning range of 10° to 80°. Bragg's equation (equation 3.2) was used to calculate the relationship between the angle of diffraction (2θ) and the distance between two planes (D-spacing) (d).

Bragg's equation

$$(2sin\theta = n\lambda \ldots\ldots\ldots\ldots\ldots\ldots\ldots\ldots \text{equ}(3.1)$$

$$d = \frac{n\lambda}{2sin\theta} \ldots\ldots\ldots\ldots\ldots\ldots\ldots\ldots equ(3.2)$$

Where: d= Spacing, n= order of diffraction, = wave length of incident X-ray (0.15406 nm), n= order of diffraction (1) and = diffraction angle.

Scherrer equation

The Scherrer equation (3.3) was utilized to determine the mean crystalline or grain size of the particle.

$$D = \frac{K\lambda}{\beta cos\theta} \ldots\ldots\ldots\ldots\ldots\ldots\ldots\ldots \text{equ (3.3)}$$

Where, D= Crystallite size, K= shape factor (Scherrer constant) (0.9), = wave length of X-ray (0.15406 nm), = Full width half maxima (FWHM), = diffraction angle.

3.5.3. Thermo-gravimetric analysis (TGA)

TGA was applied for thermal analysis to observe the physical and chemical properties of materials which are measured as a function of a temperature rise. Thermo gravimetric analysis (TGA)/derivative thermo gravimetric (DTG) is a device for collecting data regarding the degradation of the thermal material (Gao et al., 2012). TGA is helpful in the determination of biochar thermal stability.

3.5.4. Brunauer-Emmett-Teller Analysis (BET)

The surface area of biochar was examined using BET analysis. The study of surface area is important because this property of biochar is mainly responsible for pollutant removal from soil and aqueous environment.

3.6. Adsorption: Include kinetic, isotherm studies

Adsorption has been found to be one of the most effective and established treatment of wastewater in textile industry as it is an economically achievable process for dyes removal and/or decolorization of textile effluents. The process involves the transfer of soluble dyes from wastewater to the surface of the adsorbent which is solid and highly porous material. The adsorbent adsorbs each compound to be removed to its capacity and it is spent should be replaced by fresh material.

3.6.1. Bath experiment

The batch experiments of the adsorption were conducted at room temperature (25°C) in a 250 mL conical flask. In this experiment 0.2, 0.4, 0.6, 0.8, 1.0, 1.2 g of the adsorbent dosage was weighed and placed in the flask containing 50 mL CR dye solution. The suspension was stirred for interval of time between 10–210 min. i.e. 10, 50, 90, 130, 170, 210, min using a magnetic agitator and stirrer at a controllable speed. After agitation, the suspensions were filtered using Whatman no. 1 filter paper. The concentration of the filtrate was determined by using a UV-visible spectrophotometer. The absorbance was measured at the 515nm absorption wavelength.

Color removal efficiency can be as:

$\eta = \frac{C_o - Ct)}{C_o} 100\%$.....equ (3.4)

Where C_t= concentration of adsorb ate at time ´t´

C_o=initial concentration

Adsorption capacity $(q) = \frac{C_o - C_e}{m} V$ ... ... $equ(3.5)$

Where, C_o- Initial concentration in mg/g,

C_e - Concentration at equilibrium,

m - Mass of the adsorbent,

V is the volume of solution containing solute (adsorbate)

3.6.2. Adsorption kinetics

Adsorption kinetics study is essential for waste water purification since it offers helpful insights into reaction forms, adsorption reaction mechanisms, and process characteristics. Based on chemical reaction kinetics, pseudo-first order and pseudo-second order kinetic models primarily described the adsorption process (Azizian, 2004).

Table3.1 .Equation for pseudo-first and pseudo-second order kinetic models

Isotherm model	Equation	Plot	Reference
Pseudo1st order	$log(q_e - q_t) = logq_e - K_1/2.303t$	$log(q_e - q_t) vs\ t$	(Wong, et al 2004)
Pseudo 2nd order	$t/q = t/K_2 q_{e2} + t/q_e$	$t/q_t\ vs\ t$	(Ho, 2009)

3.6.3. Adsorption Models

The equilibrium model used to characterize equilibrium behavior by describing the amount of adsorbate adsorbed as a function of gas or liquid concentration at constant temperature is called isotherm (Al-Ghouti, et al. 2020). The basis of the study of the adsorption process is the adsorption isotherm model. The adsorption isotherm is the main source for measuring adsorption of substances.

Several equilibrium models have been used to explain the adsorption process, such as Langmuir, Freundlich adsorption Temkin, Hill, Rdke-Prausnitz, and Flory-Huggins

isotherms. Langmuir and Freundlich adsorption adsorption are the most commonly used models (Chen, 2015).

Langmuir assumes that the surface of the adsorbent for removing adsorbate is uniform and flat, and adsorbed molecules or ions have no interaction. On the other hand the Freundlich model assumes that the adsorption occurs on uneven surface, each local adsorption site has its binding energy, and the strongest binding site is established before the end of adsorption process (Chen, et al 2015).

Table 3.2. Equations for Langmuir, Freundlich and Temkin isotherm models.

Isotherm model	Non-linear equation	Linear equation	plot	Reference
Langmuir	$\frac{q_{e=q_{max}} bC_e}{1+bC_e}$	$\frac{C_e}{q_e} = \frac{1}{bq_{max}} + \frac{1}{q_{max}} C_e$	$\frac{C_e}{q_e}\ vs C_e$	(Swenson, 2019).
Freundlich	$q_{e=K_F} C_e \frac{1}{n}$	$logq_{t=logK_F} + \frac{1}{n} C_e$	$lnq_e vs\ lnC_e$	(Shikuku, 2018)
Temkin		$q_{e=\frac{R_T}{B}} lnK_{T+\frac{R_T}{b}} lnC_e$	$lnK_T\ vs\ lnC_e$	(Ayawei,et al.,2017)

According to Ayawei et al. (2017), the Temkin isotherm model can be used to relate the effects of indirect adsorbate/adsorbate interactions on the adsorption process. It is also assumed that as the surface area increases, all molecules in the layer's heat of adsorption will decrease linearly. By ignoring the extremely low and large values of concentrations, the model assumes that the heat of adsorption (function of temperature) of all molecules within the layer would decrease linearly rather than logarithmically with coverage (Dada et al., 2021). This isotherm includes an aspect that explicitly takes into consideration the adsorbent – adsorbate interactions. The following equations provide the Temkin isotherm model's linear form. The slope and intercept of the qe were used to calculate the adsorption parameters (A_T and β).

Langmuir model

$$\frac{C_e}{q_e} = \frac{1}{bq_{max}} + \frac{1}{q_{max}}C_e \ldots\ldots\ldots\ldots\ldots\ldots\ldots\ldots\ldots\ldots\ldots\ldots\ldots\ldots\ldots\ldots\ldots\ldots\ldots\ldots\ldots.\ldots\ldots..equ(3.6)$$

Freundlich model

$$logq_t = logK_F + \frac{1}{n}C_e \ldots\ldots\ldots\ldots\ldots\ldots\ldots\ldots\ldots\ldots\ldots\ldots.\ldots\ldots\ldots\ldots\ldots..equ(3.7)$$

Where K and K_F are the Langmuir binding term related to interaction energies (L/mg) and the Freundlich affinity coefficient ((mg/g)(1/mg)$_{1/n}$), respectively. q_{max} is the Langmuir maximum capacity(mg/g), C_e is the equilibrium solution concentration(mg/L) of the adsorbate, and n is the Freundlich linearity constant.

Temkin isotherm model

$$q_e = \frac{R_T}{b_t} lnA_T + \frac{R_T}{b_T} lnC_e \ldots\ldots\ldots\ldots\ldots\ldots\ldots\ldots\ldots\ldots\ldots\ldots\ldots\ldots\ldots\ldots.\ldots\ldots\ldots.\ldots\ldots e.qu(3.8)$$

$$q_e = \beta lnA_T + \beta lnC_e \ldots\ldots\ldots\ldots\ldots\ldots\ldots\ldots\ldots\ldots\ldots\ldots\ldots\ldots\ldots\ldots\ldots\ldots\ldots\ldots\ldots\ldots.equ(3.9)$$

where A_T is Temkin isotherm equilibrium binding constant (L/g), bT is Temkin isotherm constant, R is the universal gas constant (8.314J/mol.k), T is the temperature (298 k) and, β is constantly related to the heat of adsorption (J/mol).

3.7. Regeneration experiment

Regeneration studies are typically used to recover the depleted adsorbent and to clarify the adsorption mechanism (Yu et al., 2011).There were three solutions used in this study: solution of hydrochloric acid, deionized water, and sodium hydroxide solution. To evaluate the effectiveness of various desorption solutions study, the solute concentration was fixed at 0.01 M (apart from the distilled water. If the dye molecules desorbed by deionized water, weak bonds typically dominate the adsorption process, if not, ion exchange dominates the adsorption process and it is desorbed by acid (Chen et al., 2011).

CHAPTER FOUR

RESULTS AND DISCUSSION

4.1. Characterizations of WHBC and GCWHBC

4.1.1. X-ray Diffraction Analysis

X-ray diffraction analysis (XRD) utilizes the position, intensity, and quantity of diffraction lines, along with other characteristics of crystals, to determine the phases of crystalline substances (Xu, 2016). The successful modification of WHBC is demonstrated through the comparative X-ray diffraction (XRD) analysis of WHBC and GCWHBC, as illustrated in Figure 4.1 shows the XRD spectra of WHBC and fig 4.2 shows the XRD spectra of GCWHBC. The peak observed at 2θ = 28.62° for WHBC and the peaks at 2θ = 26.4° is for GCWHBC, and 26.4° for GCWHBC after adsorption. The emergence of a new peak at 2θ = 20.18° indicates the formation of GCWHBC.

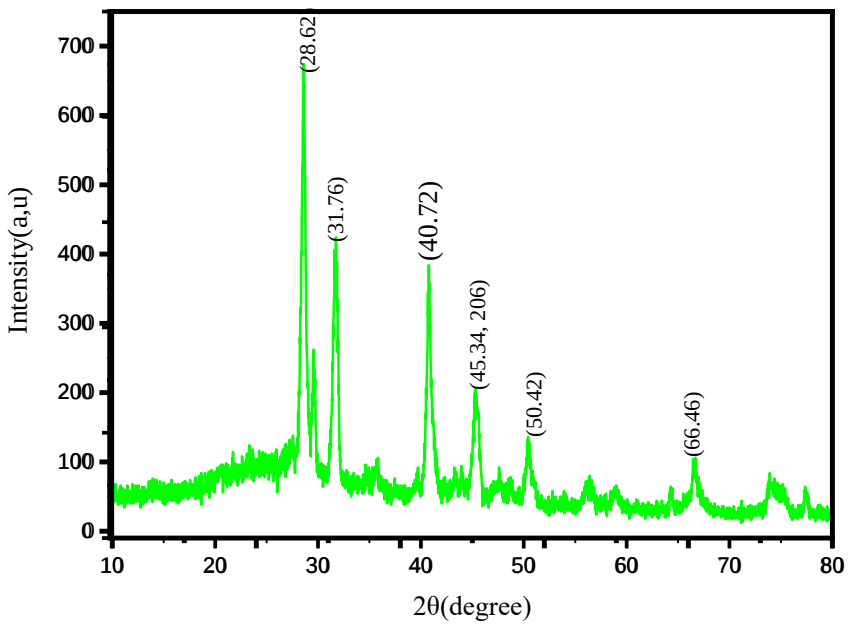

Figure 4. 1.XRD spectra of WHBC

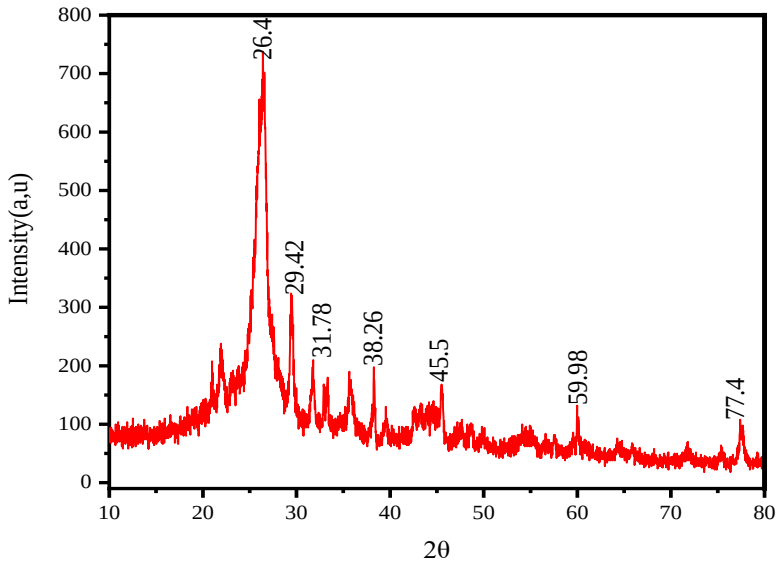

Figure 4. 2.XRD spectra of GCWHBC

Figures 4.1 and 4.2 allow for an important observation - the peak positions for water hyacinth biochar are at higher 2θ values than those of graphene-containing water hyacinth biochar. This implies that the unmodified biochar possesses greater crystallinity than the modified biochar, suggesting the graphene incorporation changed the original structure of the water hyacinth biochar.

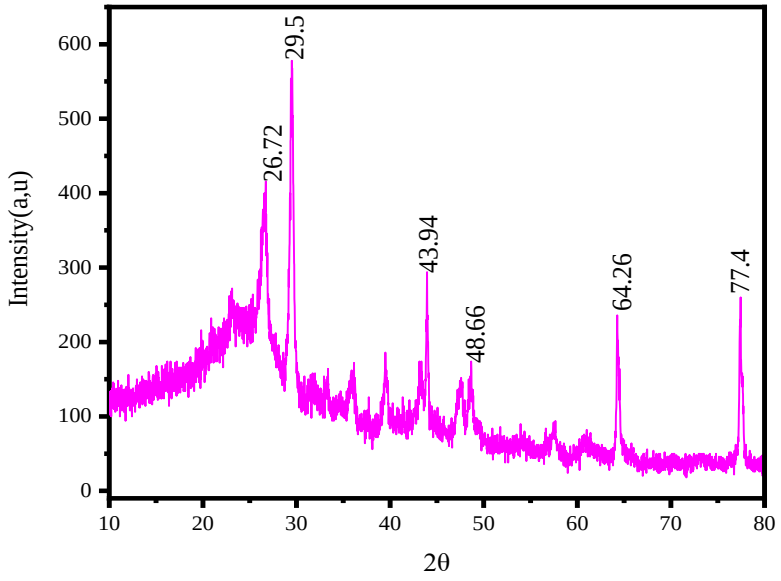

Figure 4. 3. XRD spectra of GCWHBC after adsorption

The XRD results indicate that the peak positions for graphene-containing biochar before and after adsorption are quite similar, suggesting little structural deterioration of GCWHBC occurred as a result of the adsorption process. The maintenance of the crystalline structure provides insight into GCWHBC's reusability potential.

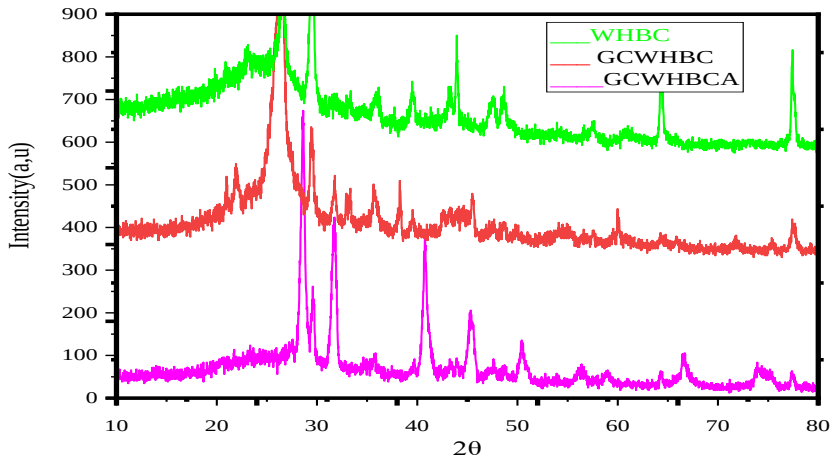

Figure 4. 4. XRD spectra of WHBC, GCWGBC before and after adsorption

4.1.2. Fourier Transform Infrared (FTIR) spectroscopy

Fourier transform infrared (FTIR) spectroscopy is a vibrational technique that can be used to examine the functional groups present on biochar surfaces. The FTIR spectroscopy revealed significant alterations to the biochar as the temperature increased during production, resulting in changes to the mixture and bonding/structural arrangements on the biochar (Yaashikaa et al., 2020).

The surface functional groups of WHBC biochar were determined using FTIR spectroscopy both before and after CR dyes were adsorbed. Before adsorption, the WHBC biochar sample's broad band at 3344 cm^{-1} indicates the stretching vibration of the O-H hydroxyl functional groups. It is the C=O stretching vibration of the carbonyl groups that causes the prominent peaks at 1581 cm^{-1}. The stretching vibration of aromatic C=C bonds corresponds to this peak, indicating the possibility of aromatic compounds. The bending vibration of methyl ($-CH_3$) groups or the stretching vibration of C-N bonds is indicated by the sharp peaks found at 1409 cm^{-1}.

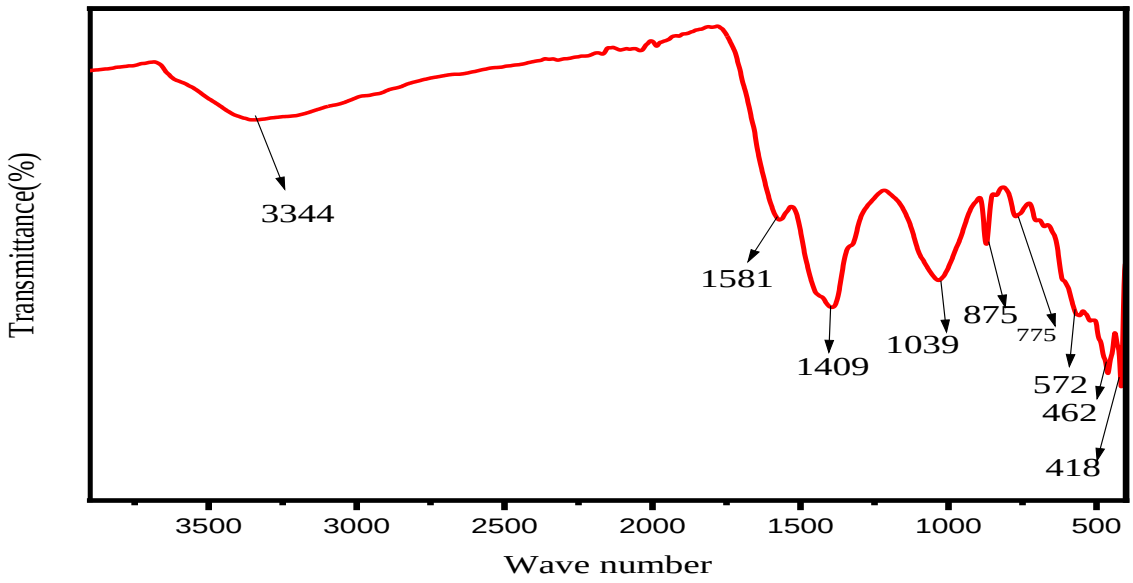

Figure 4. 5. FTIR analysis before before modification

At 1039 peak can be indicative of C-O stretching vibrations, suggesting the presence of alcohols. At 875 this peak corresponds to the stretching vibration of C-H bonds, which could be present in various organic compounds. The peak at 775 cm^{-1} may suggest the

presence of C-Cl stretching vibrations, indicating the presence of chlorinated organic compounds. Peak at 572 cm^{-1} can be associated with C-S stretching vibrations, suggesting the presence of sulfur-containing compounds. Peak at 642 cm^{-1}: This peak corresponds to the bending vibration of aromatic C-H bonds, further indicating the presence of aromatic compounds.

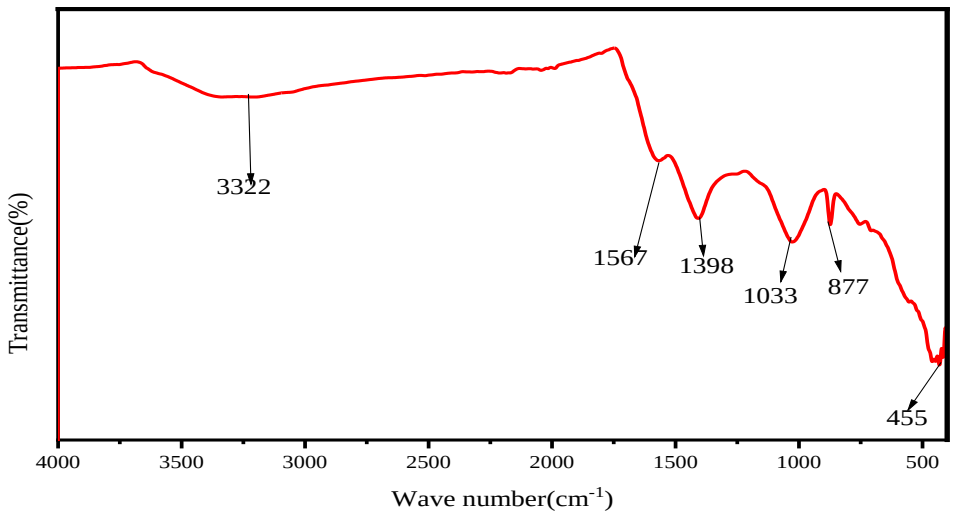

Figure 4. 6. FTIR spectra of GCWHBC before adsorption

Peak at 1567 cm^{-1}: This peak corresponds to the stretching vibration of sp^2 hybridized carbon atoms, which is characteristic of graphene. This peak is often associated with the C=C stretching vibrations in aromatic rings.

Peak at 1398 cm^{-1}: This peak can be attributed to the stretching vibration of C-O bonds, suggesting the presence of alcohols, ethers, or esters.

Peak at 1033 cm^{-1}: This peak can indicate the presence of C-O stretching vibrations, suggesting the presence of alcohols, ethers, or esters.

Peak at 877 cm^{-1}: This peak corresponds to the stretching vibrations of C-H bonds, which could be present in various organic compounds.

Peak at 455 cm^{-1}: This peak may suggest the presence of out-of-plane bending vibrations of C-H bonds in aromatic compounds. The results of the FTIR analysis appear consistent

with previous findings reported (xu et al., 2016), validating the interpretation of the spectroscopic data. Such agreement with previous research supports the findings made about the surface functional groups and bonding arrangements found on the biochar samples.

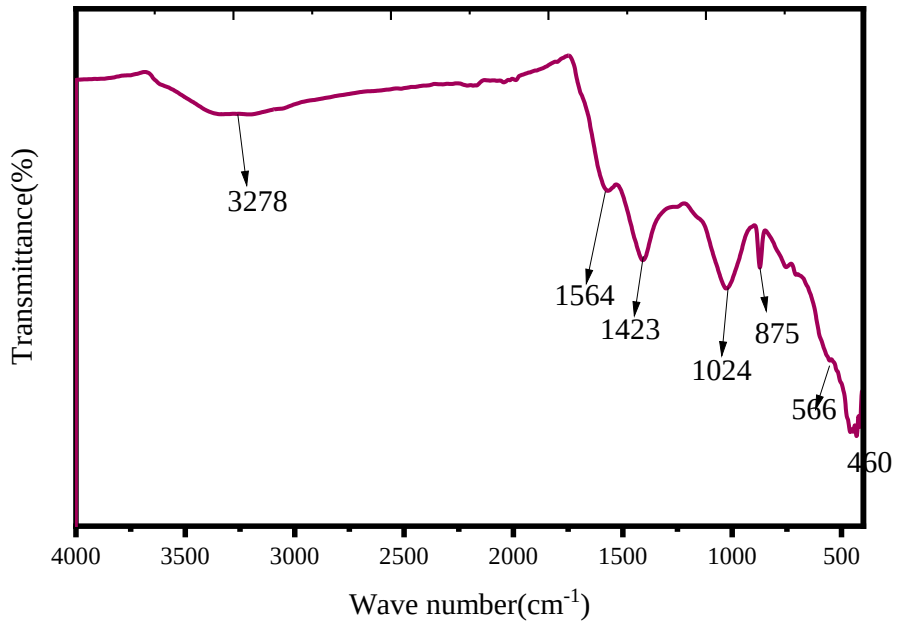

Figure 4. 7. FTIR spectra of GCWHBC after adsorption

At 3278 cm^{-1} this peak is likely associated with the presence of O-H stretching vibrations, indicating the presence of hydroxyl groups (alcohols or phenols) or water molecules. 1564 cm^{-1} peak corresponds to the C=C stretching vibration, indicating the presence of aromatic or conjugated double bonds. 1423 cm^{-1} peak could be associated with C-H bending vibrations, indicating the presence of alkane or alkene groups.

1024 cm^{-1} peak can be attributed to C-O stretching vibrations, suggesting the presence of alcohol, ether, or ester functional groups. 875 cm-1 peak might correspond to C-H bending vibrations in aromatic compounds. 566 cm^{-1}: This peak is likely associated with C-Cl stretching vibrations, indicating the presence of chlorinated compounds. The peak observed at 460 cm^{-1} could reasonably be associated with out of plane bending vibrations of aromatic rings. Such vibrational modes are commonly detected via FTIR spectroscopy for compounds containing aromatic moieties.

Nevertheless, it was evident that following the CR adsorption, the hydroxyl and carbonyl peaks (3322 and 1398 cm^{-1}) of GCWHWB shifted to a higher frequency at 3378 and 1423cm^{-1}, respectively, with increased peak intensity. These modifications might result from the unique ways that carboxyl and hydroxyl groups interact with CR molecules.

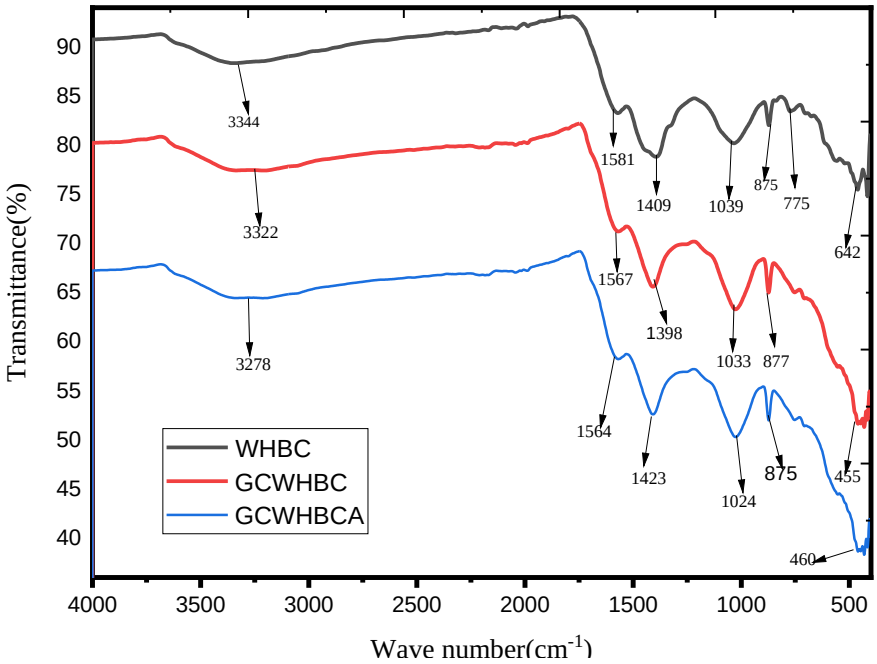

Figure 4. 8. FTIR spectra of WHBC, GCWHBC and GCWHBC after adsorption

4.1.3. Brunauer-Emmett-Teller (BET) Analysis

The surface area of water hyacinth biochar and graphene containing water hyacinth biochar was determined by BET analysis. The study of surface area of biochar is very important because this property is responsible for removal of wastes or contaminants, including textile wastes. Table shows the result of BET analysis, accordingly the specific surface area of WHBC is 297.2 m^2/g while the specific surface area of GCWHBC is 375.5 m^2/g. The increment in the specific surface area is due to modification by graphene which possess high specific surface area. This result is confirms the works of (Fang,et al.,2020).

Table 4. 1. Result of BET analysis

Sample	Surface area(m^2/g)
Water hyacinth biochar	297.2
Graphene containing water hyacinth biochar	373.5

4.1.4. Thermogravimetric analysis of water hyacinth

Thermogravimetric analysis, or TGA for short, is a method used in chemistry and materials science to examine a substance's thermal characteristics. It involves monitoring a sample's weight changes as it is heated or cooled under carefully monitored circumstances. A thermogravimetric analyzer (TGA) was used to examine the thermal properties of cellulose fibers in a nitrogen atmosphere, operating in the temperature range of 100 to 800 ◦C. Figure 10 displays the results of the thermogravimetric analysis of water hyacinth.

84.087% is the highest weight that was recorded (Fig. 4.8). There are four distinct stages, as can be seen in the figure: stage 1 is up to 250°C, stage 2 is from 250 to 340°C and involves a 60% weight loss, and stage 3 involves WHFs. The reduction phase of the hemicellulose and glycosidic links of cellulose causes the degradation of WHFs at 140–270 °C (Sumrith et al., 2020); at stage 3, the subsequent degradation happens at 320°C and continues to 430°C with a 52% weight loss percentage. According to Packiam et al. (2022), this behavior is caused by lignin degradation, which happens above 400°C. The remaining portion, part 4, has a temperature range of 430 to 520°C and a 46% weight loss.

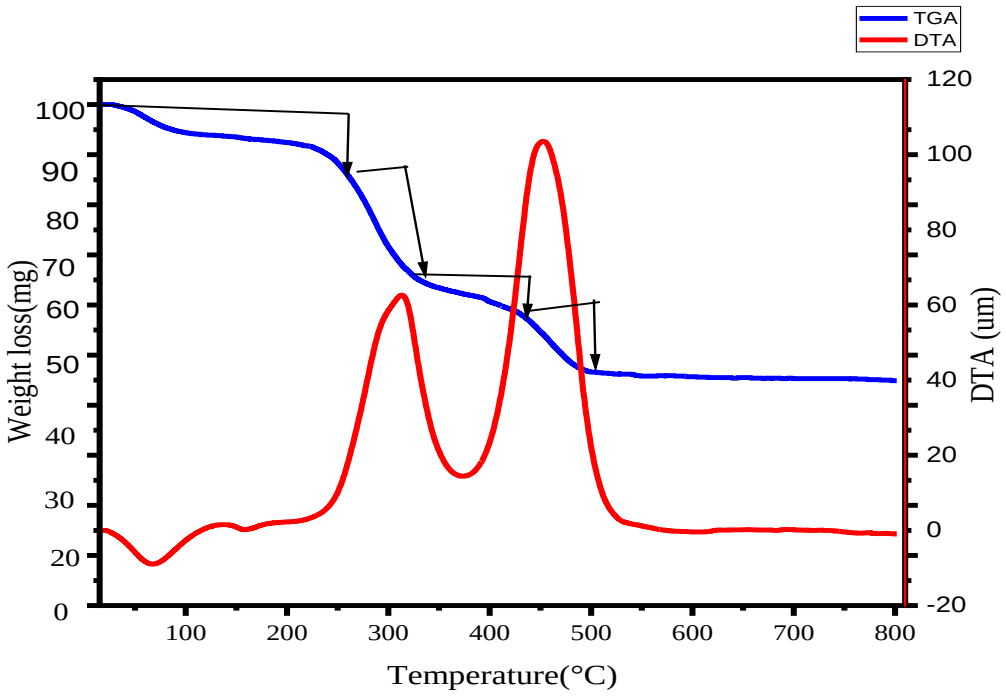

Figure 4.9. Thermogravimetric analysis of raw water hyacinth

4.2. Effects of operating parameters on adsorption efficiency

4.2.1. Effect of Adsorbent dosage

In this section the effect of adsorbent dosage on adsorption efficacy is studied. In this experiment, different amounts of adsorbents (0.2–1.0 g) were added to a 60 mg/L C R solution. Afterwards, the solution is placed in the shaker for 150min; at room temperature and natural pH: pH of CR dye. In the early stages of the batch experiment, the percentage adsorption of CR increased with increasing GCWHBC dosage. This could be because raising the adsorbent dose increases the number of active sites available during CR adsorption (Extross, et al., 2023). Fig. 1 illustrates how GCWHBC dosages affect CR adsorption. The ideal dosage of GCWHBC for CR was found to be 1 g/60 ml of CR dye solution. Beyond saturation point, increasing the GCWHBC dosage has no effect on the removal of CR.

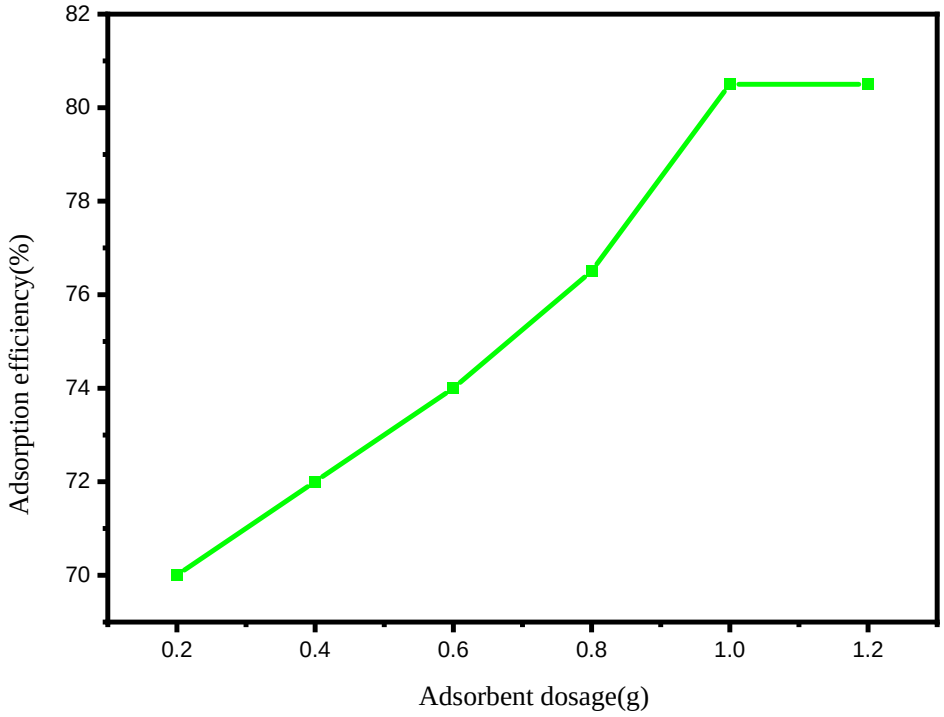

Figure 4.10. Effect of adsorbent dosage on adsorption efficiency

Therefore, it was determined that 1 g/60 mL was the ideal dosage, and this value was applied to for further experiments. The observation revealed that GCWHBC (80.5%) was adsorbed. Some reports claim that CR GCWHBC has a higher adsorption rate than other adsorbents. Of these, (68%) reported by Dbik et al. (2020), (79%) by Kulkarni et al. (2021).

4.2.2. Effect of contact time

To investigate and comprehend the equilibrium time of the adsorption process and the amount of dye adsorbed at various time intervals with a given adsorbent dosage, studies pertaining to the effect of contact time are important. The difference in CR removal for 50 mL of CR solution at different contact durations (30–210 min) and adsorbent doses of 1g/50 mL with initial concentration 50mg/L were observed. For this study, the pH of CR in its natural condition was considered. Fig. 2 shows how contact time affects the removal of CR.

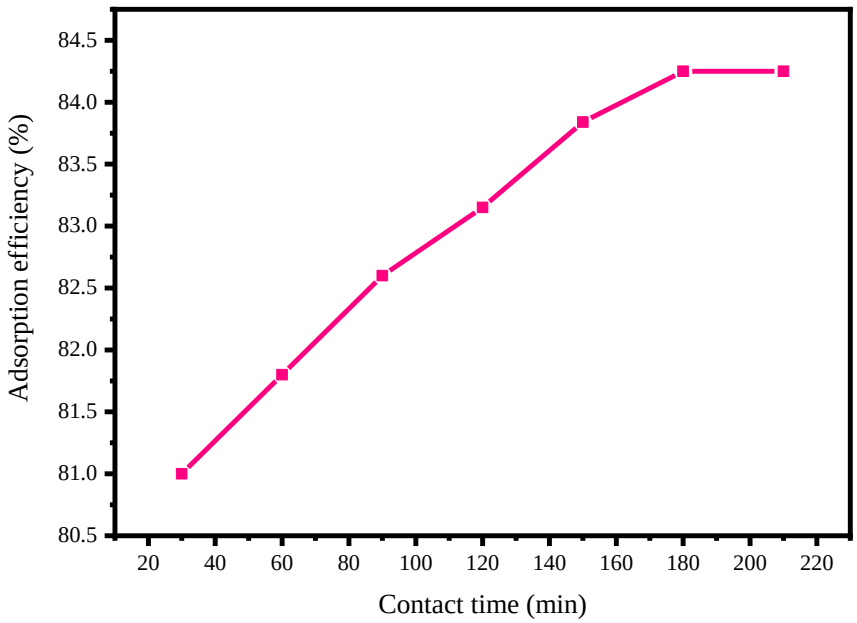

Figure 4.11. Effect of contact time.

The maximum adsorption efficiency achieved was 84.25% at 180 minutes. After this time, there was no further increment in adsorption efficiency, indicating that equilibrium had been reached and 180 minutes represented the equilibrium time for this level of adsorption efficiency.

4.2.3. Effect of initial concentration

In order to study the effect of the initial dye concentration onto GCWHBC, various concentrations of CR 20,40,60,80 and 100ppm were selected. Figure 6 shows how the initial concentration of CR affects the removal efficiency of CR onto GCWHBC. After 180min of equilibrium adsorption time, the removal of dye molecules drops from 88.1 to 68.39% with an increase in the initial concentration of CR from 20 to 100 ppm. Because the total number of binding sites on the surface of GCWHBC was restricted for a given dosage of GCWGBC, the efficiency of removing CR decreased as the initial concentration of CR increased. The percentage of removal decreased with increasing

initial dye concentration. Adsorbate removal decreases in proportion to an increase in initial adsorbate concentration (adsorbent saturation) for a given adsorbent dose because the total number of available adsorption sites is fixed, adsorbing nearly the same amount of adsorbate. Other researchers also reported similar results. (Xu, et al., 2016).

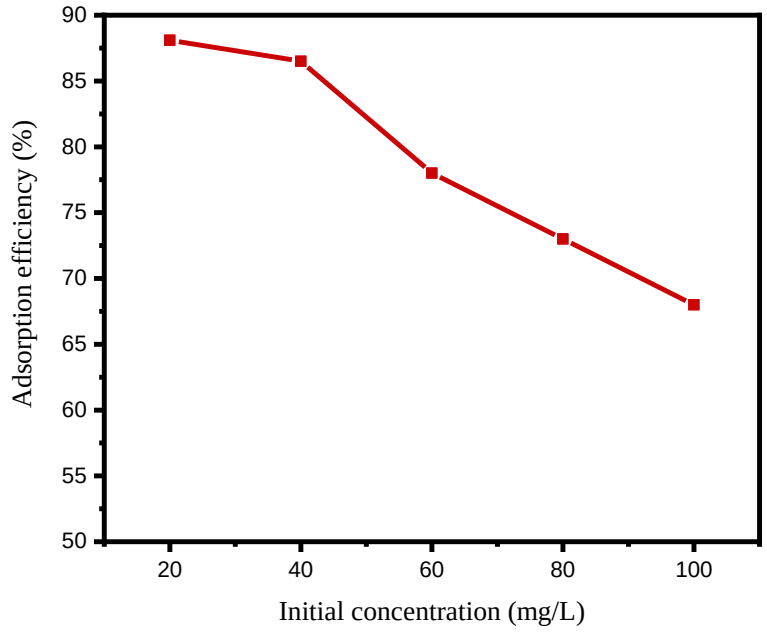

Figure 4.12. Effect of initial concentration

The study was conducted using the adsorbent dose of 1g /50 mL for duration of 180 minutes, at the natural pH of CR.

4.2.4. Determination of point of zero charge (pzc)

The point of zero charge (pHpzc) methodology refers to a point at which the surface charge of the adsorbent is neutral (Carneiro, 2023). NaOH solutions (0.1 mol /Land 0.1 mol/ L) of HCl were used to adjust the pH. A pH meter was used to take the reading. The mixtures were stirred for 24 hours at 150 revolutions per minute at 25 ºC. The pH was then measured both before and after stirring. The initial pH was recorded as pH_0, and the final pH as pHf.

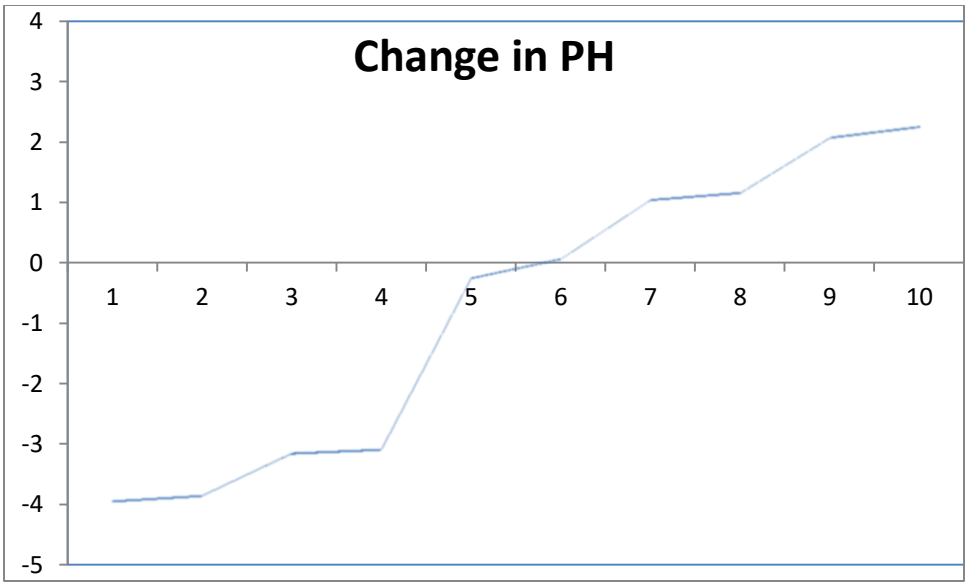

Figure 4.13. Point of zero charge (pzc)

As shown on the graph above, the point of zero charge was 6. Because of the negative charge on the biochar's surface and the excess OH ions in the solution, which compete for sorption sites, the sorption of an anionic dye decreases as pH rises. The surface of the biochar becomes protonated when pH < pHzpc, which causes dye molecules to compete for the available sites (Laxmi, et al., 2023).

4.2.5. Effect of PH

The pH of the solution has a significant impact on the adsorption process, especially on the adsorption efficiency. It is considered as an important controlling parameter that has the potential to have a big impact on the adsorption process. The adsorbent's surface binding sites and the dye molecule's ionization process are both affected by the pH of the solution (Jeyavishnu and Alagesan 2020). To achieve maximum adsorption of Congo red onto adsorbent, an optimum pH plays an important role in the process of adsorption. The effect of pH from 2 to 12 was studied for a fixed duration of time (180min), with a constant dye concentration of 20 mg/L and a constant adsorbent dose of 1 g/50mL. The results were plotted as adsorption efficiency vs. pH in the Fig. 5. Figure 5 illustrates that the removal of CR remained nearly constant within the pH range of 3–6. After pH 6 the removal of CR drops from 90.6 to 78.43% up to pH 12. The literature revealed that other

adsorbents such as orange peel activated by microwave (Yek et al. 2020), coffee waste AC (Lafi et al. 2019), showed maximum adsorption of congo red dye in the range of 2-6.

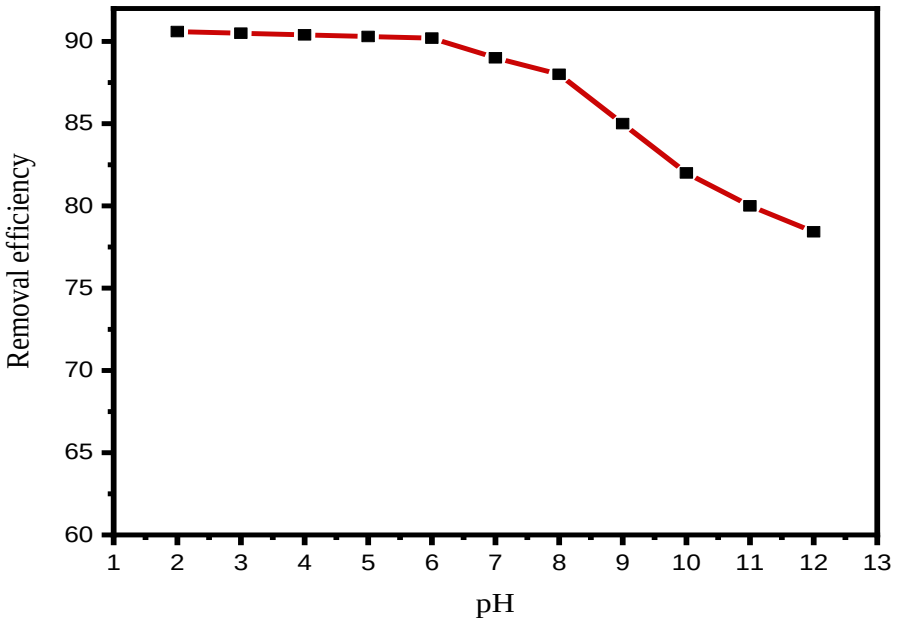

Figure 4.14. Effect of pH

4.3. Adsorption isotherm studies

The equilibrium model used to characterize equilibrium behavior by describing the amount of adsorbate adsorbed as a function of gas or liquid concentration at constant temperature is called isotherm (Al-Ghouti, et al. 2020). The basis of the study of the adsorption process is the adsorption isotherm model. The adsorption isotherm is the main source for measuring adsorption of substances.

The adsorption isotherm indicates how the adsorbate molecules are distributed between the liquid and solid phases when the adsorption process is in the equilibrium state (Yang, 2016). An analysis of the fitness between the data and different isotherm models is an important step in determining the suitable model. Three well-known models, including the Langmuir, Freundlich and Temkin isotherms, have been selected to explain the dye-

biochar interactions observed in this study. These three isotherm equations' linear forms are given as follows:

$$\frac{C_e}{q_e}=\frac{1}{bq_{max}}+\frac{Ce}{q_{max}} \quad \text{.....1}$$

$$lnq_e = LogK_F + \frac{1}{n}LogC_e \quad \text{.....2}$$

$$q_e = B_T lnA_T + B_T lnC_e \quad \text{.....3}$$

Where q_e(mg/g) is the equilibrium adsorption capacity , q_{max}(mg/g) is maximum adsorption capacity, b(l/mg) is the Langmuir adsorption constant and C_e is the equilibrium concentration , K_F is the Freundlich constant [(mg/g)(1/g)1/n], n is adsorption intensity, A and B are the Temkin constant.

4.3.1. Langmuir isotherm

The maximum adsorption capacity (q_{max}) and energy of adsorption (K_L) of the Langmuir isotherm model were determined to be 51.28205 mg/g and 0.196513 L/mg respectively. The correlation factor (R^2) for the Langmuir isotherm yielded a value of 0.99413.

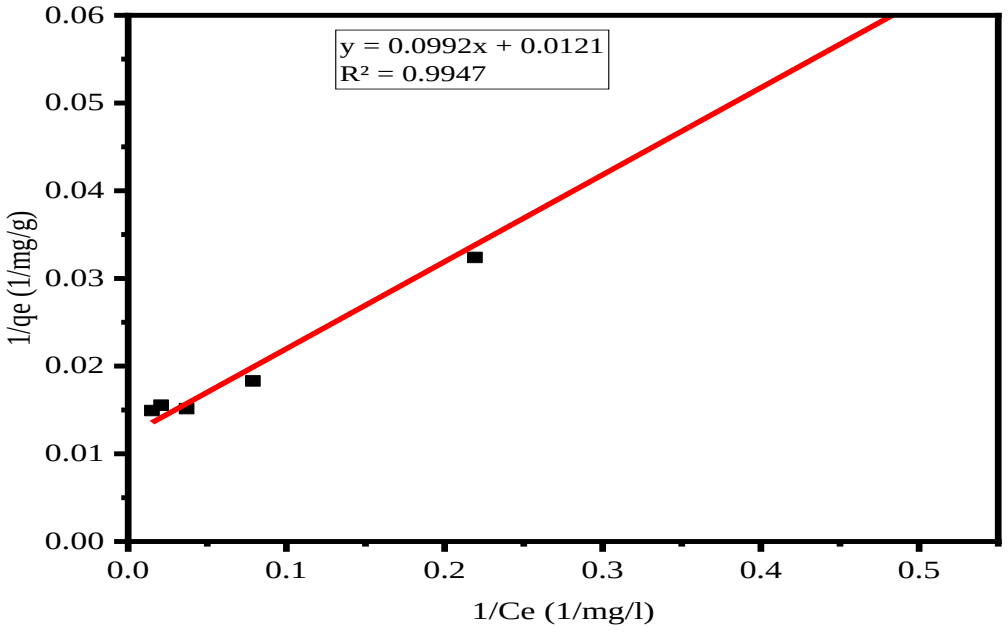

Figure 4.15. Langmuir isotherm

The maximum adsorption capacity (q_{max}) and energy of adsorption (K_L) of the Langmuir isotherm model were determined to be 51.28205 mg/g and 0.196513 L/mg respectively. The correlation factor (R^2) for the Langmuir isotherm yielded a value of 0.99413. The Langmuir isotherm model is the most appropriate and well-fitting model, as indicated by the proximity of the R^2 values to unity indicating mono-layer adsorption and the adsorption mechanism is chemisorption.

Table 4. 2. Adsorption isotherms data

Experiment no	C_i	C_e	$1/c_e$	$Logc_e$	Lnc_e	q_e	$1/q_e$	$Logq_e$
1	10	2	0.5	0.30103	0.693147	16	0.0625	1.20412
2	20	4.56	0.219298	0.658965	1.517323	30.88	0.032383	1.489677
3	40	12.68	0.078864	1.103119	2.540026	54.64	0.018302	1.737511
4	60	27	0.037037	1.431364	3.295837	66	0.015152	1.819544
5	80	47.84	0.020903	1.679791	3.867862	64.32	0.015547	1.808346
6	100	66.5	0.015038	1.822822	4.197202	67	0.014925	1.826075

4.3.2. Freundlich model

The main assumption from the Freundlich isotherm is that the adsorbent sites have an exponential distribution as a result of multilayer adsorption. In this case, the adsorbate that has been adsorbed serves as an additional adsorbent, hastening the adsorption process. This process takes place in a heterogeneous surface (Jeyavishnu, et a., 2020).

Not every dot is being touched by the line. This means that this model does not fit the experimental data.

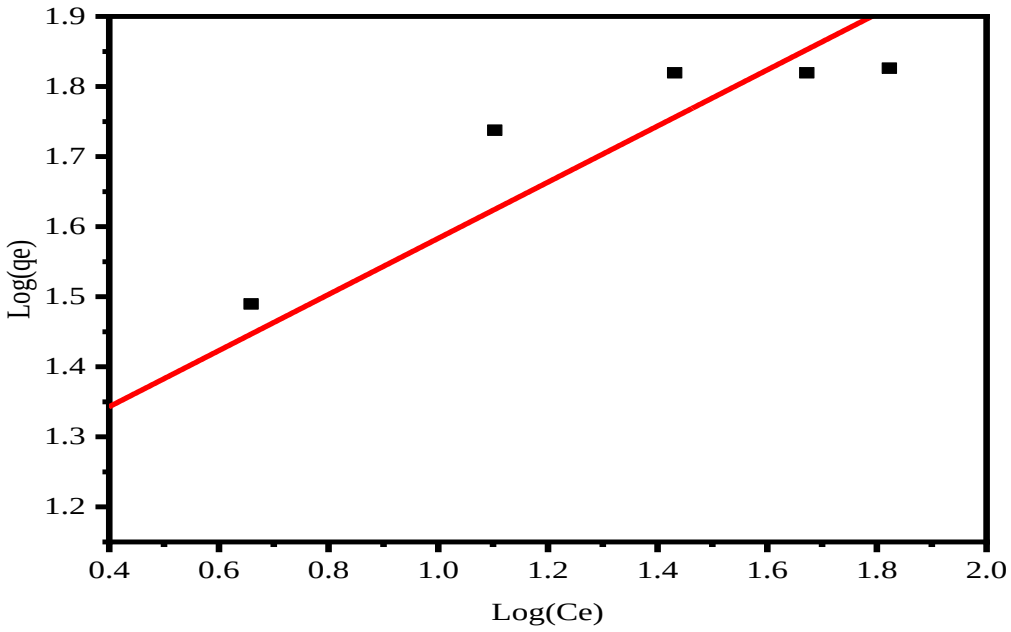

Figure 4.16. Freundlich isotherm

4.3.3. Temkin isotherm

Assumption made from this isotherm is decrease of heat of sorption is linear rather than being logarithmic due to adsorbate and adsorbent interaction (Jeyavishnu, & Alagesan, 2020). The Temkin isotherm can be expressed mathematically as in Eq. (3), where A_T (L/mg) is the binding constant and B represents the heat of adsorption. Correlation coefficient R^2 for Temkin isotherm was found to be near unity (0.93251) which is lower than the Langmuir isotherm.

Table 4. 3. Adsorption isotherm's parameters and values

Isotherm	Isotherm parameters	Value
Langmuir	q_{max} (mg/g)	51.28205 mg/g
	K_L (L/mg)	0.196513
	R^2	0.99413.
Freundlich	n	2.50897
	1/n	0.39857
	kf (mg/g)(1/mg)1/n	15.236
	R^2	0.85956

Temkin	B_T	15.185
	A_T (L/mg)	1.81158
	R^2	0.93251

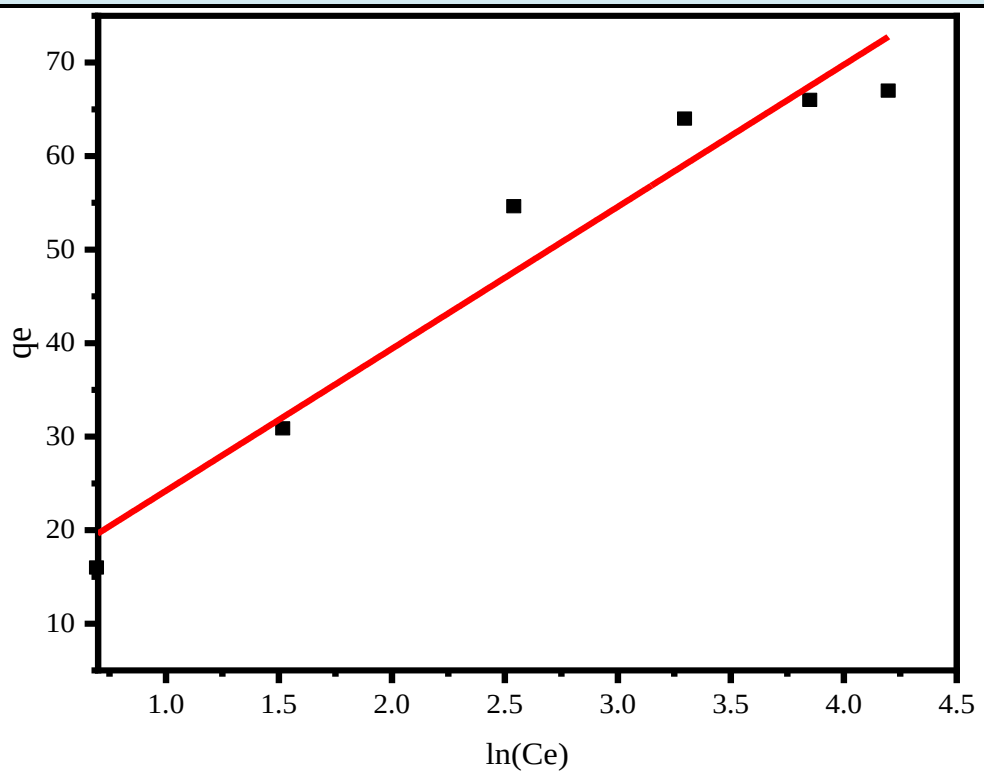

Figure 4.17. Temkin isotherm

4.4. Kinetic Study

Adsorption kinetics is one of the most important factors to investigate when studying an adsorption system. This is because the rate at which adsorption takes place is ultimately determined by the kinetics. The kinetics of adsorption is determined by the surface area of the adsorbent, flow rates, and solute concentration. Physical and chemical adsorptions are the two main types of adsorption; at a given adsorbent concentration. Figure 17 illustrates how contact time affects the dyes' adsorption by biochars. The dyes are quickly adsorbed at first. Thereafter, the adsorption gradually increases over time, reaching equilibrium at 180 minutes. The experiment was conducted with pH equal to 4, an initial CR concentration of 40 mg/L, and an adsorbent dosage of 1 g/L at constant room temperature. Adsorption kinetics models, i.e. Weber–Morris, PSO and PFO, are used to

understand adsorbate-adsorbent interactions in the present study (Extross et al., 2023).

$ln(q_e - q_t) = lnq_e - K_1 t$.....4

$\frac{t}{q_t} = \frac{1}{K_1 q_e 2} + \frac{1}{q_e}$.....5

Intercept	Slope	q_e(mg/g)	k_1	R^2
-0.77241	-0.03051	0.461899	-0.00017	0.62659

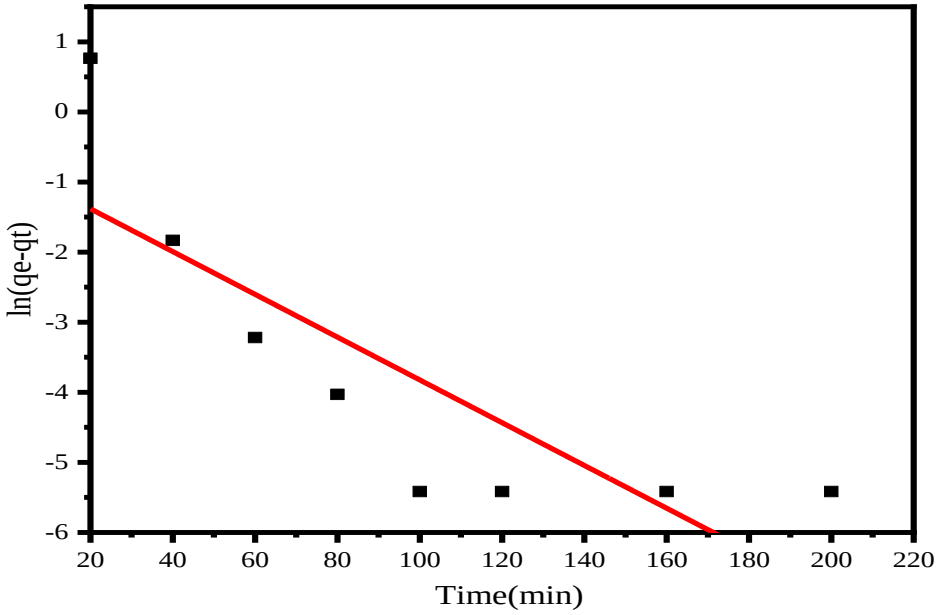

Figure 4.18. Pseudo 1st order

From figure 18, it is observed that the dots on the graph are not touched by the line and the R^2 is 0.62659. This implies that first order kinetic model is not suitable for this experimental data.

Intercept	slope	q_e(mg/g)	qe^2	k_2	R^2
0.10265	0.01551	64.47453	4156.966	0.002343	0.99423

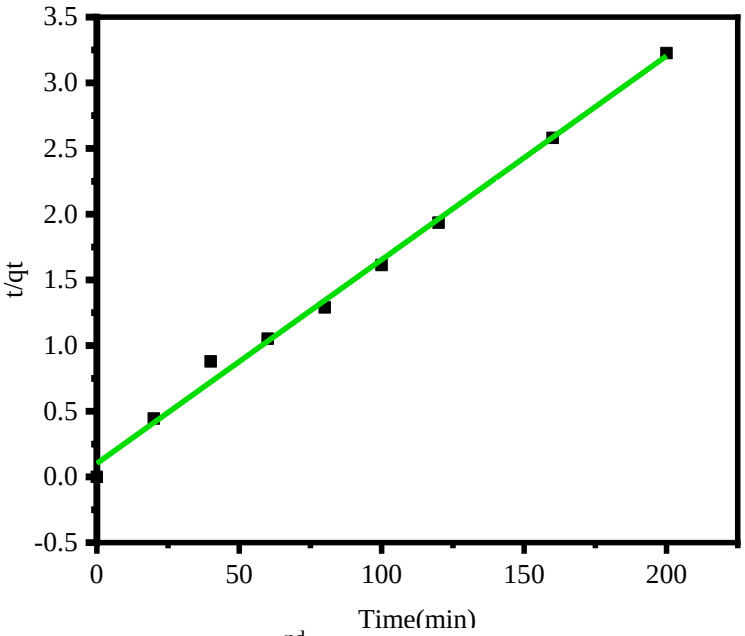

Figure 4.19. Pseudo 2nd order

The table above demonstrates that the PSO model exhibits an R^2 value that is closest to unity, indicating that the second-order kinetic model best describes the adsorption of CR dye according to these data.

4.5. Removal of dyes from real textile industry wastewater

In order to put the results of the laboratory experiment into a useful real-world application, the synthetic GCWHBC was tested to remove CR dye from the textile wastewater. The study on the environmental application of GCWHBC to actual textile industry effluent was investigated by adding 1.0 g of GCWHBC to 40 ml of industrial effluent collected from a textile industry found in Adama industrial park. By adding 1.0 mg of GCWHBC to 40 mL of industrial effluent collected from a textile industry in Adama industrial park. The concentration of CR dye in real textile water is 65.8 mg/L, as determined by UV-vis spectroscopy at 515 nm with a pH of 6 at room temperature for 24 hours. The study on the environmental application of GCWHBC to actual textile industry effluent was investigated. After filtering the samples, the CR concentrations were measured using UV-vis spectrophotometer. The removal efficiency of GCWHBC was found to be 63.2%.

It notes that GCWHBC achieved a removal efficiency of 63.2% for CR dye from actual textile wastewater. While lower than the efficiency observed in synthetic wastewater by

24.9%, this decrease is reasonably attributed to competitive species interference naturally present in real industrial effluent. The adsorbent also tested by another textile dyes methylene blue and methyl orange. The concentration of textile effluents containing methylene blue and methyl orange are 18.2 and 31 mg/L respectively as it was measured by the above method. The removal efficiencies of both dyes are 62 and 58% respectively.

4.6. Regeneration experiment

Biochar and modified biochar gradually lose their reactivity when pollutants cover their active adsorption sites. Some treatments are required in order to get it back to its active state. Compared to other materials, biochar is more environmentally friendly because it can be reused. The opposite of the adsorption process is the regeneration of adsorbents. To increase the efficiency of the adsorption cycle, regeneration is necessary. For industrial uses, a good adsorbent should be recyclable and reusable. As a result of this repeated adsorption-desorption process, the cost of biochar adsorbents would be greatly reduced. With continued application, biochar's adsorption effectiveness may decline. Thermal regeneration, solvent regeneration, microwave irradiation regeneration, and supercritical fluid regeneration are the four primary methods of biochar regeneration (Aziz, 2023).When it comes to adsorbing Congo Red dye using water hyacinth biochar, an appropriate solvent for regeneration can be an acidic solution. Congo red is an anionic dye, and acidic conditions can help enhance the adsorption capacity of biochar for such dyes. In this case, hydrochloric acid (HCl) is used as the solvent for regeneration.

First 0.5 M HCl solution was prepared by diluting it with distilled water. Then the graphene containing water hyacinth biochar with 1g/L dosage was immersed in the acidic solution and agitated. After the regeneration process, the biochar was removed from the acidic solution and rinsed thoroughly with distilled water to remove any residual acid. This step is crucial to avoid any interference of acid residues during the adsorption process. After that the pH of the regenerated biochar was adjusted to a neutral or slightly acidic range using a dilute alkaline (sodium hydroxide). Finally, the regenerated biochar was dried in ambient conditions before using it for the adsorption of Congo red dye. This regeneration study was carried out with 40mg/L of congo red at 6 pH for 180min. Accordingly there were four successive regeneration steps. At the first step 86% removal

efficiency was achieved. The second regeneration cycle provides 82.56%, the third and fourth regeneration cycles provided 77.8% and 74% respectively. This value guarantees that there will be minimal adsorption capacity loss when the prepared adsorbent is reused multiple times.

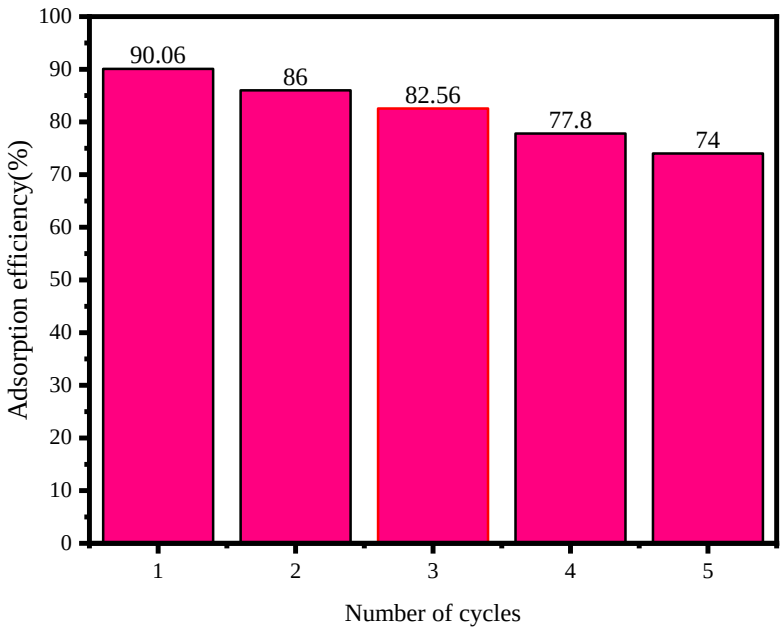

Figure 4.20. Regeneration of graphene containing water hyacinth biochar

CHAPTER FIVE

5. CONCLUSIONS AND RECOMMENDATIONS

5.1. Conclusions

From this research, the following conclusion can be drawn:

Graphene containing water hyacinth biochar is a good adsorbent for dye removal from textile waste, showing that the maximum adsorption efficiency is 90.6 %.The modification of WHBC by graphene improved the physiochemical properties of the biochar, thereby enhancing the adsorption efficiency of the adsorbent by increasing the adsorption sites of the biochar. Characterization analyses such as XRD, SEM, and FTIR reveal that dye molecules are effectively adsorbed by GCWHBC. The BET analysis result showed that the surface area of GCWHBC is 373.5 m^2/g. The adsorption mechanism involved the interaction between the hydroxyl and carbonyl groups on the surface of GCWHBC and the dye molecules. The Langmuir adsorption isotherm is best fitted for this experiment (R^2 = 0.99413), and the pseudo-second-order kinetic model is best fitted (R^2 = 0.99423). After multiple cycle adsorptions, the exhausted adsorbent could be efficiently regenerated by 0.1 mol L^{-1} HCl to maintain optimal removal ability for dyes. Even after being used to remove CR from the real dye wastewater, GCWHBC showed strong adsorption efficiency. Water hyacinth-derived graphene-modified biochar is believed to provide a new, environmentally friendly, and economically viable ad sorbent that can be widely used for dye removal from textile wastes.

5.2. Recommendations

Based on the findings of this study, the following recommendations are made for future research:

- Economic feasibility and life cycle assessment: performing an economic feasibility analysis and life cycle assessment of the production and utilization of graphene-containing water hyacinth biochar.

- Consider factors such as raw material availability, production costs, energy consumption, and environmental impacts to assess the viability and sustainability of the adsorbent.
- Comparison with other adsorbents: To compare the performance of graphene-containing water hyacinth biochar with other graphene-based materials. This comparative analysis can provide insights into the advantages and limitations of the developed adsorbent.
- Future research work should focus on determining the adsorption efficiency of this adsorbent on other contaminants in order to realize its more widespread application.

REFERENCES

Agrafioti, E., Bouras, G., Kalderis, D., & Diamadopoulos, E. (2013). Biochar production by sewage sludge pyrolysis. *Journal of analytical and applied pyrolysis*, *101*, 72-78.

Ahmad, M., Lee, S. S., Dou, X., Mohan, D., Sung, J. K., Yang, J. E., & Ok, Y. S. (2012). Effects of pyrolysis temperature on soybean stover-and peanut shell-derived biochar properties and TCE adsorption in water. *Bioresource technology*, *118*, 536-544.

Al-Ghouti, M. A., & Da'ana, D. A. (2020). Guidelines for the use and interpretation of adsorption isotherm models: A review. *Journal of hazardous materials*, *393*, 122383.

Amalina, F., Abd Razak, A. S., Krishnan, S., Zularisam, A. W., & Nasrullah, M. (2022). A comprehensive assessment of the method for producing biochar, its characterization, stability, and potential applications in regenerative economic sustainability–a review. Cleaner Materials, 3, 100045.

Amalina, F., Abd Razak, A. S., Krishnan, S., Zularisam, A. W., & Nasrullah, M. (2022). Water hyacinth (Eichhornia crassipes) for organic contaminants removal in water–A review. *Journal of Hazardous Materials Advances*, *7*, 100092.

Amalina, F., Abd Razak, A. S., Krishnan, S., Zularisam, A. W., & Nasrullah, M. (2022). Dyes removal from textile wastewater by agricultural waste as an absorbent–a review. *Cleaner Waste Systems*, 100051.

Amalina, I. F., Haziq, J. M., Syukor, A. A., Rashid, A. M., & Izzati, K. N. (2020). Formulation of Capra hircus feed to utilize Artocarpus heterophyllus leaves and palm acid oil (PAO). In *IOP Conference Series: Materials Science and Engineering* (Vol. 736, No. 2, p. 022016). IOP Publishing.

Annadurai, G., Juang, R. S., & Lee, D. J. (2002). Use of cellulose-based wastes for adsorption of dyes from aqueous solutions. *Journal of hazardous materials*, *92*(3), 263-274.

Aragaw, T. A., & Asmare, A. M. (2018). Phycoremediation of textile wastewater using indigenous microalgae. *Water Practice & Technology*, *13*(2), 274-284.

Asghar, A., Raman, A. A. A., & Daud, W. M. A. W. (2015). Advanced oxidation processes for in-situ production of hydrogen peroxide/hydroxyl radical for textile wastewater treatment: a review. *Journal of cleaner production*, *87*, 826-838.

Ayawei, N., Ebelegi, A. N., & Wankasi, D. (2017). Modelling and interpretation of adsorption isotherms. *Journal of chemistry*, *2017*.

Aziz, K. H. H., & Kareem, R. (2023). Recent advances in water remediation from toxic heavy metals using biochar as a green and efficient adsorbent: A review. *Case Studies in Chemical and Environmental Engineering*, 100495.

Azizian, S. (2004). Kinetic models of sorption: a theoretical analysis. *Journal of colloid and Interface Science*, *276*(1), 47-52.

Babuponnusami, A., & Muthukumar, K. (2014). A review on Fenton and improvements to the Fenton process for wastewater treatment. *Journal of Environmental Chemical Engineering*, *2*(1), 557-572.

Banat, F., & Al-Bastaki, N. (2004). Treating dye wastewater by an integrated process of adsorption using activated carbon and ultrafiltration. *Desalination*, *170*(1), 69-75.

Behera, M., Nayak, J., Banerjee, S., Chakrabortty, S., & Tripathy, S. K. (2021). A review on the treatment of textile industry waste effluents towards the development of efficient mitigation strategy: An integrated system design approach. *Journal of Environmental Chemical Engineering*, *9*(4), 105277.

Benkhaya, S., M'rabet, S., & El Harfi, A. (2020). A review on classifications, recent synthesis and applications of textile dyes. *Inorganic Chemistry Communications*, *115*, 107891.

Burhenne, L., & Aicher, T. (2014). Benzene removal over a fixed bed of wood char: The effect of pyrolysis temperature and activation with CO2 on the char reactivity. *Fuel processing technology*, *127*, 140-148.

Carneiro, M. T., Morais, A. Í. S., de Carvalho Melo, A. L. F., Ferreira, F. J. L., Santos, F. E. P., Viana, B. C., ... & Silva-Filho, E. C. (2023). Biochar Derived from Water Hyacinth Biomass Chemically Activated for Dye Removal in Aqueous Solution. *Sustainability*, *15*(19), 14578.

Cetin, E., Moghtaderi, B., Gupta, R., & Wall, T. F. (2004). Influence of pyrolysis conditions on the structure and gasification reactivity of biomass chars. *Fuel*, *83*(16), 2139-2150.

Chen, S., Qin, C., Wang, T., Chen, F., Li, X., Hou, H., & Zhou, M. (2019). Study on the adsorption of dyestuffs with different properties by sludge-rice husk biochar: adsorption capacity, isotherm, kinetic, thermodynamics and mechanism. *Journal of Molecular Liquids*, *285*, 62-74.

Chen, X. (2015). Modeling of experimental adsorption isotherm data. *information*, *6*(1), 14-22.

Chung, K. T. (2000). Mutagenicity and carcinogenicity of aromatic amines metabolically produced from azo dyes. *Journal of Environmental Science & Health Part C*, *18*(1), 51-74.

Chung, K. T. (2016). Azo dyes and human health: A review. *Journal of Environmental Science and Health, Part C*, *34*(4), 233-261.

Classen, J. J., Chandler, W. J., Huie, R. S., & Osborne, J. A. (2013). A centrifuge-based procedure for suspended solids measurements in Lagoon sludge. *Transactions of the ASABE*, *56*(2), 747-752.

Crini, G., & Lichtfouse, E. (2019). Advantages and disadvantages of techniques used for wastewater treatment. *Environmental Chemistry Letters*, *17*, 145-155.

Da Silva, P. M. M., Camparotto, N. G., Lira, K. T. G., Picone, C. S. F., & Prediger, P. (2020). Adsorptive removal of basic dye onto sustainable chitosan beads: Equilibrium, kinetics, stability, continuous-mode adsorption and mechanism. *Sustainable Chemistry and Pharmacy*, *18*, 100318.

Dafnopatidou, E. K., Gallios, G. P., Tsatsaroni, E. G., & Lazaridis, N. K. (2007). Reactive dyestuffs removal from aqueous solutions by flotation, possibility of water reuse, and dyestuff degradation. *Industrial & engineering chemistry research*, *46*(7), 2125-2132.

Das, O., Sarmah, A. K., & Bhattacharyya, D. (2015). Structure–mechanics property relationship of waste derived biochars. *Science of the Total Environment*, *538*, 611-620.

Dbik, A., Bentahar, S., El Khomri, M., El Messaoudi, N., & Lacherai, A. (2020). Adsorption of Congo red dye from aqueous solutions using tunics of the corm of the saffron. *Materials today: proceedings*, *22*, 134-139.

De Bhowmick, G., Sarmah, A. K., & Sen, R. (2018). Lignocellulosic biorefinery as a model for sustainable development of biofuels and value added products. *Bioresource technology*, *247*, 1144-1154.

Deaconu, M., Senin, R., Stoica, R., Athanasiu, A., Crudu, M., Oproiu, L., ... & Filipescu, C. (2016). Adsorption decolorization technique of textile/leather–dye containing effluents. *Int. J. Waste Resour*, *6*, 212-218.

Deniz, F. (2013). Adsorption properties of low-cost biomaterial derived from Prunus amygdalus L. for dye removal from water. *The Scientific World Journal*, *2013*.

Downie, A., Crosky, A., & Munroe, P. (2012). Physical properties of biochar. In *Biochar for environmental management* (pp. 45-64). Routledge.

El Mouzdahir, Y., Elmchaouri, A., Mahboub, R., Gil, A., & Korili, S. A. (2010). Equilibrium modeling for the adsorption of methylene blue from aqueous solutions on activated clay minerals. *Desalination*, *250*(1), 335-338.

Extross, A., Waknis, A., Tagad, C., Gedam, V. V., & Pathak, P. D. (2023). Adsorption of congo red using carbon from leaves and stem of water hyacinth: Equilibrium, kinetics, thermodynamic studies. *International journal of Environmental Science and Technology*, *20*(2), 1607-1644.

Fan, H., Ma, Y., Wan, J., Wang, Y., Li, Z., & Chen, Y. (2020). Adsorption properties and mechanisms of novel biomaterials from banyan aerial roots via simple modification for ciprofloxacin removal. *Science of the Total Environment*, *708*, 134630.

Fang, Z., Gao, Y., Bolan, N., Shaheen, S. M., Xu, S., Wu, X., ... & Wang, H. (2020). Conversion of biological solid waste to graphene-containing biochar for water remediation: A critical review. *Chemical Engineering Journal*, *390*, 124611.

Fang, Z., Hu, Y., Cheng, J., & Chen, Y. (2019). Continuous removal of trace bisphenol A from water by high efficacy TiO2 nanotube pillared graphene-based macrostructures in a photocatalytically fluidized bed. *Chemical Engineering Journal*, *372*, 581-589.

Faria, P. C. C., Órfão, J. J. M., & Pereira, M. F. R. (2009). Activated carbon and ceria catalysts applied to the catalytic ozonation of dyes and textile effluents. *Applied Catalysis B: Environmental*, *88*(3-4), 341-350.

Feng, Y., Zhou, H., Liu, G., Qiao, J., Wang, J., Lu, H., ... & Wu, Y. (2012). Methylene blue adsorption onto swede rape straw (Brassica napus L.) modified by tartaric acid: Equilibrium, kinetic and adsorption mechanisms. *Bioresource technology*, *125*, 138-144.

Geçgel, Ü., Özcan, G., & Gürpınar, G. Ç. (2013). Removal of methylene blue from aqueous solution by activated carbon prepared from pea shells (Pisum sativum). *Journal of Chemistry*, *2013*.

Goyal, H. B., Seal, D., & Saxena, R. C. (2008). Bio-fuels from thermochemical conversion of renewable resources: a review. *Renewable and sustainable energy reviews*, *12*(2), 504-517.

Gupta, V. K., Khamparia, S., Tyagi, I., Jaspal, D., & Malviya, A. (2015). Decolorization of mixture of dyes: A critical review.

Hao, O. J., Kim, H., & Chiang, P. C. (2000). Decolorization of wastewater. *Critical reviews in environmental science and technology*, *30*(4), 449-505.

Hoslett, J., Ghazal, H., Ahmad, D., & Jouhara, H. (2019). Removal of copper ions from aqueous solution using low temperature biochar derived from the pyrolysis of municipal solid waste. *Science of the total environment*, *673*, 777-789.

Hussain, S., Van Leeuwen, J., Chow, C., Beecham, S., Kamruzzaman, M., Wang, D.,& Aryal, R. (2013). Removal of organic contaminants from river and reservoir waters by three different aluminum-based metal salts: Coagulation adsorption and kinetics studies. *Chemical Engineering Journal*, *225*, 394-405.

Hussein, F. H. (2013). Chemical Properties of Treated Textile Dyeing Wastewater. *Asian Journal of Chemistry*, *25*(16).

Hynes, N. R. J., Kumar, J. S., Kamyab, H., Sujana, J. A. J., Al-Khashman, O. A., Kuslu, Y., ... & Kumar, B. S. (2020). Modern enabling techniques and adsorbents based dye removal with sustainability concerns in textile industrial sector-A comprehensive review. *Journal of cleaner production*, *272*, 122636.

Jadhav, A. J., & Srivastava, V. C. (2013). Adsorbed solution theory based modeling of binary adsorption of nitrobenzene, aniline and phenol onto granulated activated carbon. *Chemical engineering journal*, *229*, 450-459.

Jain, R., Mathur, M., Sikarwar, S., & Mittal, A. (2007). Removal of the hazardous dye rhodamine B through photocatalytic and adsorption treatments. *Journal of environmental management*, *85*(4), 956-964.

Jamee, R., & Siddique, R. (2019). Biodegradation of synthetic dyes of textile effluent by microorganisms: an environmentally and economically sustainable approach. *European journal of microbiology and immunology*, *9*(4), 114-118.

Jeyavishnu, K., & Alagesan, V. (2020). Cereus sp. as potential biosorbent for removal of Congo red from aqueous solution: isotherm and kinetic investigations. *Environmental monitoring and assessment*, *192*, 1-15.

Ji, P., Zhang, J., Chen, F., & Anpo, M. (2009). Study of adsorption and degradation of acid orange 7 on the surface of CeO2 under visible light irradiation. *Applied Catalysis B: Environmental*, *85*(3-4), 148-154.

Kadhom, M., Albayati, N., Alalwan, H., & Al-Furaiji, M. (2020). Removal of dyes by agricultural waste. *Sustainable Chemistry and Pharmacy*, *16*, 100259.

Kant, R. (2012). Textile dyeing industry an environmental hazard. J Nat Sci 4 (1): 22–26.

Khan, R., Patel, V., & Khan, Z. (2020). Bioremediation of dyes from textile and dye manufacturing industry effluent. In *Abatement of Environmental Pollutants* (pp. 107-125). Elsevier.

Kiran, S., Ali, S., & Asgher, M. (2013). Degradation and mineralization of azo dye reactive blue 222 by sequential photo-Fenton's oxidation followed by aerobic biological treatment using white rot fungi. *Bulletin of environmental contamination and toxicology*, *90*, 208-215.

Kulkarni, R. M., Vaidya, R., Srinivas, S., Anand, S., & Narayana, B. (2021). Application of water hyacinth root powder for Congo red dye removal in batch and continuous packed bed operation. *Nanotechnology for Environmental Engineering*, *6*(2), 31.

Kumar, A., & Jena, H. M. (2016). Preparation and characterization of high surface area activated carbon from Fox nut (Euryale ferox) shell by chemical activation with H3PO4. *Results in Physics*, *6*, 651-658.

Lafi, R., Gzara, L., Lajimi, R. H., & Hafiane, A. (2018). Treatment of textile wastewater by a hybrid ultrafiltration/electrodialysis process. *Chemical Engineering and Processing-Process Intensification*, *132*, 105-113.

Lafi, R., Montasser, I., & Hafiane, A. (2019). Adsorption of congo red dye from aqueous solutions by prepared activated carbon with oxygen-containing functional groups and its regeneration. *Adsorption Science & Technology*, *37*(1-2), 160-181

Laxmi Deepak Bhatlu, M., Athira, P. S., Jayan, N., Barik, D., & Dennison, M. S. (2023). Preparation of Breadfruit Leaf Biochar for the Application of Congo Red Dye Removal from Aqueous Solution and Optimization of Factors by RSM-BBD. *Adsorption Science & Technology*, *2023*.

Lehmann, J., & Joseph, S. (2015). Biochar for environmental management: an introduction. In *Biochar for environmental management* (pp. 1-13). Routledge.

Li, S., Harris, S., Anandhi, A., & Chen, G. (2019). Predicting biochar properties and functions based on feedstock and pyrolysis temperature: A review and data syntheses. *Journal of Cleaner Production*, *215*, 890-902.

Liang, C. Z., Sun, S. P., Li, F. Y., Ong, Y. K., & Chung, T. S. (2014). Treatment of highly concentrated wastewater containing multiple synthetic dyes by a combined process of coagulation/flocculation and nanofiltration. *Journal of Membrane Science*, *469*, 306-315.

Liang, C., Gascó, G., Fu, S., Méndez, A., & Paz-Ferreiro, J. (2016). Biochar from pruning residues as a soil amendment: effects of pyrolysis temperature and particle size. *Soil and Tillage Research*, *164*, 3-10.

Lorenc-Grabowska, E., & Gryglewicz, G. (2007). Adsorption characteristics of Congo Red on coal-based mesoporous activated carbon. *Dyes and pigments*, *74*(1), 34-40.

Mahmoud, D. K., Salleh, M. A. M., Karim, W. A. W. A., Idris, A., & Abidin, Z. Z. (2012). Batch adsorption of basic dye using acid treated kenaf fibre char: Equilibrium, kinetic and thermodynamic studies. *Chemical Engineering Journal*, *181*, 449-457.

Malik, A. (2007). Environmental challenge vis a vis opportunity: the case of water hyacinth. *Environment international*, *33*(1), 122-138.

Marcano, D. C., Kosynkin, D. V., Berlin, J. M., Sinitskii, A., Sun, Z., Slesarev, A., ... & Tour, J. M. (2010). Improved synthesis of graphene oxide. *ACS nano*, *4*(8), 4806-4814.

Martinez-Huitle, C. A., & Ferro, S. (2006). Electrochemical oxidation of organic pollutants for the wastewater treatment: direct and indirect processes. *Chemical society reviews*, *35*(12), 1324-1340.

Martins, A., & Nunes, N. (2015). Adsorption of a textile dye on commercial activated carbon: A simple experiment to explore the role of surface chemistry and ionic strength. *Journal of Chemical Education*, *92*(1), 143-147.

Mašek, O., Budarin, V., Gronnow, M., Crombie, K., Brownsort, P., Fitzpatrick, E., & Hurst, P. (2013). Microwave and slow pyrolysis biochar—Comparison of physical and functional properties. *Journal of Analytical and Applied Pyrolysis*, *100*, 41-48.

Masto, R. E., Kumar, S., Rout, T. K., Sarkar, P., George, J., & Ram, L. C. (2013). Biochar from water hyacinth (Eichornia crassipes) and its impact on soil biological activity. *Catena*, *111*, 64-71.

Mathew, M., Desmond, R. D., & Caxton, M. (2016). Removal of methylene blue from aqueous solutions using biochar prepared from Eichhorrnia crassipes (Water Hyacinth)-molasses composite: Kinetic and equilibrium studies. *African Journal of Pure and Applied Chemistry*, *10*(6), 63-72.

McKendry, P. (2002). Energy production from biomass (part 1): overview of biomass. *Bioresource technology*, *83*(1), 37-46.

Mehta, P. (2013). Chemical treatment of textile effluents using ferric chloride as coagulant: an analysis. *Int. J. Basic Appl. Chem. Sci.*, *3*, 49-55.

Mohammadi, A., & Veisi, P. (2018). High adsorption performance of β-cyclodextrin-functionalized multi-walled carbon nanotubes for the removal of organic dyes from water and industrial wastewater. *Journal of Environmental Chemical Engineering*, *6*(4), 4634-4643.

Mukherjee, Shraboni, Priyanka Sahu, and Gopinath Halder. "Microbial remediation of fluoride-contaminated water via a novel bacterium Providencia vermicola (KX926492)." *Journal of environmental management* 204 (2017): 413-423.

Nadhini, R., Koti, V. V., Vadanasundari, V., & Rangabhashiyam, S. (2012). Decolourization studies of synthetic textile dye using Aspergillus species under static and shaking conditions. *Asian J. Sci. Technol*, *4*(11), 80-82.

Nedjai, R., Alam, M. Z., & Kabbashi, N. A. (2021). Adsorption of methylene blue onto activated carbon developed from baobab fruit shell by chemical activation: Kinetic equilibrium studies. *IIUM Engineering Journal*, *22*(2), 31-49.

Nyoo, J., Ju, Y., & Edi, F. (2021). Biosorption of dyes. *Green Chemistry and Water Remediation: Research and Applications*, *10*.

Packiam, K. K., Murugesan, B., Kaliyannan Sundaramoorthy, P. M., Srinivasan, H., & Dhanasekaran, K. (2022). Extraction, purification and characterization of nanocrystalline cellulose from Eichhornia crassipes (Mart.) Solms: A common aquatic weed water Hyacinth. *Journal of Natural Fibers*, *19*(14), 7424-7435.

Pandey, A., Singh, P., & Iyengar, L. (2007). Bacterial decolorization and degradation of azo dyes. *International biodeterioration & biodegradation*, *59*(2), 73-84.

Patel, S. K., Patel, S. G., & Patel, G. V. (2020). Degradation of reactive dye in aqueous solution by Fenton, photo-Fenton process and combination process with activated charcoal and TiO 2. *Proceedings of the National Academy of Sciences, India Section A: Physical Sciences*, *90*, 579-591.

Poulose, A. M., Elnour, A. Y., Anis, A., Shaikh, H., Al-Zahrani, S. M., George, J., ... & Sarmah, A. K. (2018). Date palm biochar-polymer composites: An investigation

of electrical, mechanical, thermal and rheological characteristics. *Science of the total environment*, *619*, 311-318.

Ratna, D., Khan, S., Barman, S., & Chakraborty, B. C. (2012). Synthesis of vinylester-clay nanocomposites: Influence of the nature of clay on mechanical, thermal and barrier properties. *The Open Macromolecules Journal*, *6*(1).

Reddy, S. N., Ding, N., Nanda, S., Dalai, A. K., & Kozinski, J. A. (2014). Supercritical water gasification of biomass in diamond anvil cells and fluidized beds. *Biofuels, Bioproducts and Biorefining*, *8*(5), 728-737.

Rezania, S., Ponraj, M., Din, M. F. M., Songip, A. R., Sairan, F. M., & Chelliapan, S. (2015). The diverse applications of water hyacinth with main focus on sustainable energy and production for new era: An overview. *Renewable and Sustainable Energy Reviews*, *41*, 943-954.

Robinson, T., McMullan, G., Marchant, R., & Nigam, P. (2001). Remediation of dyes in textile effluent: a critical review on current treatment technologies with a proposed alternative. *Bioresource technology*, *77*(3), 247-255.

Saxena, M., Sharma, N., & Saxena, R. (2020). Highly efficient and rapid removal of a toxic dye: adsorption kinetics, isotherm, and mechanism studies on functionalized multiwalled carbon nanotubes. *Surfaces and Interfaces*, *21*, 100639.

Senan, R. C., & Abraham, T. E. (2004). Bioremediation of textile azo dyes by aerobic bacterial consortium aerobic degradation of selected azo dyes by bacterial consortium. *Biodegradation*, *15*, 275-280.

Shen, Y. S., Wang, S. L., Tzou, Y. M., Yan, Y. Y., & Kuan, W. H. (2012). Removal of hexavalent Cr by coconut coir and derived chars–the effect of surface functionality. *Bioresource technology*, *104*, 165-172.

Sirajudheen, P., Karthikeyan, P., Vigneshwaran, S., & Meenakshi, S. (2020). Synthesis and characterization of La (III) supported carboxymethylcellulose-clay composite for toxic dyes removal: Evaluation of adsorption kinetics, isotherms and

thermodynamics. *International journal of biological macromolecules*, *161*, 1117-1126.

Solmaz, S. K. A., Üstün, G. E., Birgül, A., & Taşdemir, Y. (2007). Treatability studies with chemical precipitation and ion exchange for an organized industrial district (OID) effluent in Bursa, Turkey. *Desalination*, *217*(1-3), 301-312.

Srebrenkoska, V., Zhezhova, S., Risteski, S., & Golomeova, S. (2014). Methods for waste waters treatment in textile industry.

Srivatsav, P., Bhargav, B. S., Shanmugasundaram, V., Arun, J., Gopinath, K. P., & Bhatnagar, A. (2020). Biochar as an eco-friendly and economical adsorbent for the removal of colorants (dyes) from aqueous environment: A review. *Water*, *12*(12), 3561.

Stroud, A. (1994). Water hyacinth (Eichhornia crassipes [Mart.] Solms) in Ethiopia.

Sumrith, N., Techawinyutham, L., Sanjay, M. R., Dangtungee, R., & Siengchin, S. (2020). Characterization of alkaline and silane treated fibers of 'water hyacinth plants' and reinforcement of 'water hyacinth fibers' with bioepoxy to develop fully biobased sustainable ecofriendly composites. *Journal of Polymers and the Environment*, *28*, 2749-2760.

Suryawan, I. W. K., Helmy, Q., & Notodarmojo, S. (2018, January). Textile wastewater treatment: colour and COD removal of reactive black-5 by ozonation. In *IOP conference series: earth and environmental science* (Vol. 106, p. 012102). IOP Publishing.

Tan, X., Liu, Y., Zeng, G., Wang, X., Hu, X., Gu, Y., & Yang, Z. (2015). Application of biochar for the removal of pollutants from aqueous solutions. *Chemosphere*, *125*, 70-85.

Tewabe, D., Asmare, E., Zelalem, W., & Mohamed, B. (2017). Identification of impacts, some biology of water hyacinth (Eichhornia crassipes) and its management options in Lake Tana, Ethiopia. *Net Journal of Agricultural Science*, *5*(1), 8-15.

Tripathi, M., Sahu, J. N., & Ganesan, P. (2016). Effect of process parameters on production of biochar from biomass waste through pyrolysis: A review. *Renewable and sustainable energy reviews*, *55*, 467-481.

Vijayaraghavan, K., & Ashokkumar, T. (2017). Plant-mediated biosynthesis of metallic nanoparticles: A review of literature, factors affecting synthesis, characterization techniques and applications. *Journal of environmental chemical engineering*, *5*(5), 4866-4883.

Walsh, M. E., Perlack, R. L., Turhollow, A., de la Torre Ugarte, D., Becker, D. A., Graham, R. L., ... & Ray, D. E. (2000). *Biomass feedstock availability in the United States: 1999 state level analysis*. EERE Publication and Product Library, Washington, DC (United States).

Wang, J. L., & Xu, L. J. (2012). Advanced oxidation processes for wastewater treatment: formation of hydroxyl radical and application. *Critical reviews in environmental science and technology*, *42*(3), 251-325.

Wang, Q., Chen, C., Zhao, D., Ma, W., & Zhao, J. (2008). Change of adsorption modes of dyes on fluorinated TiO2 and its effect on photocatalytic degradation of dyes under visible irradiation. *Langmuir*, *24*(14), 7338-7345.

Woolf, D., Amonette, J. E., Street-Perrott, F. A., Lehmann, J., & Joseph, S. (2010). Sustainable biochar to mitigate global climate change. *Nature communications*, *1*(1), 56.

Xiao, X., Chen, B., & Zhu, L. (2014). Transformation, morphology, and dissolution of silicon and carbon in rice straw-derived biochars under different pyrolytic temperatures. *Environmental science & technology*, *48*(6), 3411-3419.

Xu, Y., Liu, Y., Liu, S., Tan, X., Zeng, G., Zeng, W., ... & Zheng, B. (2016). Enhanced adsorption of methylene blue by citric acid modification of biochar derived from water hyacinth (Eichornia crassipes). *Environmental Science and Pollution Research*, *23*, 23606-23618.

Yaashikaa, P. R., Kumar, P. S., Varjani, S., & Saravanan, A. (2020). A critical review on the biochar production techniques, characterization, stability and applications for circular bioeconomy. *Biotechnology Reports*, *28*, 00570.

Yagub, M. T., Sen, T. K., Afroze, S., & Ang, H. M. (2014). Dye and its removal from aqueous solution by adsorption: a review. *Advances in colloid and interface science*, *209*, 172-184.

Yang, G., Wu, L., Xian, Q., Shen, F., Wu, J., & Zhang, Y. (2016). Removal of congo red and methylene blue from aqueous solutions by vermicompost-derived biochars. *PLoS One*, *11*(5), e0154562.

Yek, P. N. Y., Peng, W., Wong, C. C., Liew, R. K., Ho, Y. L., Mahari, W. A. W., ... & Lam, S. S. (2020). Engineered biochar via microwave CO2 and steam pyrolysis to treat carcinogenic Congo red dye. *Journal of hazardous materials*, *395*, 122636.

Yu, X. Y., Luo, T., Zhang, Y. X., Jia, Y., Zhu, B. J., Fu, X. C., ... & Huang, X. J. (2011). Adsorption of lead (II) on O2-plasma-oxidized multiwalled carbon nanotubes: thermodynamics, kinetics, and desorption. *ACS Applied Materials & Interfaces*, *3*(7), 2585-2593.

Zhang, J., Wei, Y., & Fang, Z. (2019). Ozone pollution: a major health hazard worldwide. *Frontiers in immunology*, *10*, 2518.

Zhao, G., Li, J., Ren, X., Chen, C., & Wang, X. (2011). Few-layered graphene oxide nanosheets as superior sorbents for heavy metal ion pollution management. *Environmental science & technology*, *45*(24), 10454-10462.

Zheng, Y., Hou, X., Ma, X., Hao, Z., & Ma, Z. (2021). Vitamin C-assisted fabrication of aerogels from industrial graphene oxide for gaseous hexamethyldisiloxane adsorption. *Applied Sciences*, *11*(18), 8486.

Zhou, Y., Lu, J., Zhou, Y., & Liu, Y. (2019). Recent advances for dyes removal using novel adsorbents: A review. Environmental pollution, 252, 352-365.

Zubair, M., Ihsanullah, I., Aziz, H. A., Ahmad, M. A., & Al-Harthi, M. A. (2021). Sustainable wastewater treatment by biochar/layered double hydroxide composites: Progress, challenges, and outlook. *Bioresource technology*, *319*, 124128.

APPENDIX

Appendix A: Yield of biochar

The yield of biochar can be calculated by determining the mass of biochar obtained from a given amount of feedstock used in the pyrolysis process. The yield is typically expressed as a percentage or a ratio.

Yield = (Mass of Biochar / Mass of Feedstock) × 100

In order to calculate the yield of WHBC initial mass water hyacinth biomass was 8g in each of the crucible and the mass after formation of biochar(after pyrolysis was 6.043g. So the yield of biochar can be calculated as

Yield=$\frac{6.043g}{8g}$*100=36.7%

Appendix B: Calibration curve

10	0.221
20	0.335
30	0.521
40	0.792
50	1.032

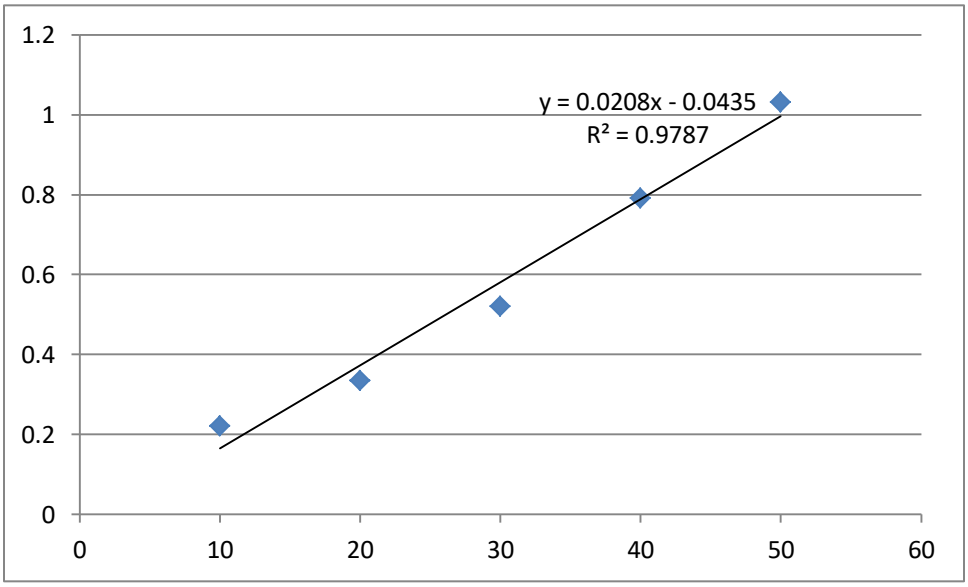

Appendix C: Biochar production at different Stages


Washing with deionized water


356
Modifying with graphene


Modified sample after drying


Stuart
60
200
Adsorption experiment

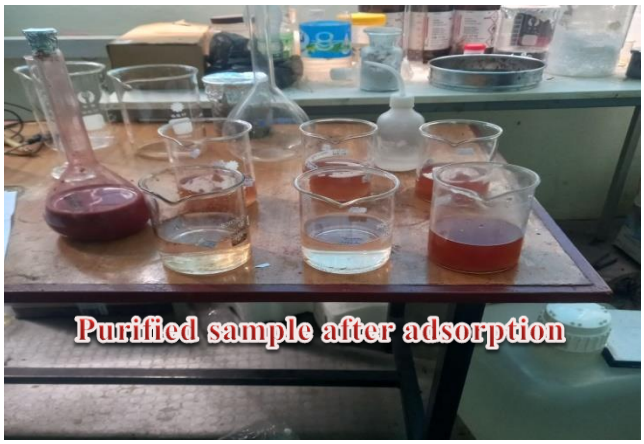
Purified sample after adsorption


Preparation of sample for
UV-VIS spectroscopy

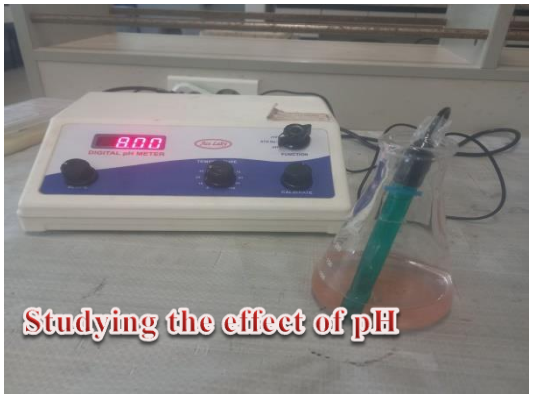

Appendix D: Isotherm data

Langmuir isotherm data

Experiment no	C_i	C_e	$1/C_e$	$\log C_e$	$\ln C_e$	q_e	$1/q_e$	$\log q_e$
1	10	2	0.5	0.30103	0.693147	16	0.0625	1.20412
2	20	4.56	0.219298	0.658965	1.517323	30.88	0.032383	1.489677
3	40	12.68	0.078864	1.103119	2.540026	54.64	0.018302	1.737511
4	60	27	0.037037	1.431364	3.295837	64	0.015625	1.80618
5	80	47	0.021277	1.672098	3.850148	66	0.015152	1.819544
6	100	66.5	0.015038	1.822822	4.197202	67	0.014925	1.826075

$$qe = \frac{Ci - Ce}{W} * V \quad , \quad \frac{1}{qe} = \frac{1}{KLqmax} * \frac{1}{Ce} + \frac{1}{qmax} \quad , \quad qmax = \frac{1}{intercept}$$

$$RL = \frac{1}{1 + Ci * KL} \quad , \quad KL = \frac{1}{slope * qmax}$$

Intercept	slope	qmax(mg/g)	KL	RL	R^2
0.0195	0.09923	51.28205	0.196513	0.11286	0.99413

Freundlich isotherm data

Experiment no	Ci	Ce	1/ce	logce	lnce	Qe	1/qe	logqe
1	10	2	0.5	0.30103	0.693147	16	0.0625	1.20412
2	20	4.56	0.219298	0.658965	1.517323	30.88	0.032383	1.489677
3	40	12.68	0.078864	1.103119	2.540026	54.64	0.018302	1.737511
4	60	27	0.037037	1.431364	3.295837	64	0.015625	1.80618
5	80	47	0.021277	1.672098	3.850148	66	0.015152	1.819544
6	100	66.5	0.015038	1.822822	4.197202	67	0.014925	1.826075

$$qe = \frac{Ci - Ce}{W} * V, \quad \frac{1}{qe} = \frac{1}{KLqmax} * \frac{1}{Ce} + \frac{1}{qmax}, \quad RL = \frac{1}{1 + Ci * KL},$$

$$qmax = \frac{1}{intercept}, \quad KL = \frac{1}{slope * qmax},$$

Intercept	slope	qmax(mg/g)	K_L	R_L	R^2
0.0195	0.09923	51.28205	0.196513	0.11286	0.99413

Temkin isotherm data

1	10	2	0.5	0.30103	0.693147	16	0.0625	1.20412
2	20	4.56	0.219298	0.658965	1.517323	30.88	0.032383	1.489677
3	40	12.68	0.078864	1.103119	0.416947	54.64	0.018302	1.737511
4	60	27	0.037037	1.431364	3.295837	66	0.015152	1.819544
5	80	47	0.021277	1.672098	3.850148	66	0.015152	1.819544
6	100	66.5	0.015038	1.822822	4.197202	67	0.014925	1.826075

$$qe = \frac{RT}{bT} lnAT + \frac{RT}{bT} lnCe$$

Appendix E: Kinetics data

Pseudo first order

Experiment no	Ci(mg/l)	Ce(mg/l)	qe(mg/g)
1	10	2	16
2	20	4.56	33
3	40	12.68	54.64
4	60	27	55
5	80	47	66
6	100	66.5	67

$$qe = \frac{Ci - Ce}{W} * V$$

Experiment no	Time(min)	Cimg(/l)	Ce(mg/l)	qt(mg/g)	ln(qe-qt)
1	0	0	0	0	0
2	20	40	20.3	45	0.765985
3	40	40	19.5	45.5	-1.83258
4	60	40	19.3	64	-3.21888
5	80	40	19.1	66.5	-4.02981
6	100	40	18.8	66.501	-5.4161
7	120	40	18.8	42.4	-5.4161
8	160	40	18.8	42.4	-5.4161
	200				-5.4161

$$ln(qe - qt) = lnqe - k1t$$

,

Intercept=lnqe, qe=anintln of intercept value
Slope=k1t,,,,,,k1=slope/t

Pseudo 2nd order data

experiment no	Ci(mg/l)	Ce(mg/l)	qe(mg/g)
1	10	2	16
2	20	4.56	33
3	40	12.68	54.64
4	60	27	55
5	80	47	66
6	100	66.5	67

$$qe\frac{=Ci-Ce}{W}*V \quad , \frac{t}{qe}=\frac{1}{k1qe2}+\frac{1}{qe},$$

graph=t vs t/qt

slope=1/qe,,,qe=1/slope,

intercept=1/k2qe^2,,,,k2=1/intercept*qe^2

intercept	slope	qe(mg/g)	qe^2	k2	R^2
0.10265	0.01551	64.47453	4156.966	0.002343	0.99423

Experiment no	Time(min)	Cimg(/l)	Ce(mg/l)	qt(mg/g)	ln(qe-qt)
1	0	0	0	0	0
2	20	40	20.3	45	0.765985
3	40	40	19.5	45.5	-1.83258
4	60	40	19.3	57	-3.21888
5	80	40	19.1	62	-4.02981
6	100	40	18.8	62	-5.4161
7	120	40	18.8	62	-5.4161
8	160	40	18.8	62	-5.4161
9	200	40	18.8	62	-5.4161